

USING THE DOWNHOLE SEISMIC AND CROSSHOLE SEISMIC TECHNIQUES  
TO MEASURE SOIL STRESS ANISOTROPY IN THE FIELD

by

IAN J. PILKINGTON

A THESIS SUBMITTED IN PARTIAL FULFILMENT OF  
THE REQUIREMENTS FOR THE DEGREE OF  
GEOLOGICAL ENGINEERING

in

THE FACULTY OF APPLIED SCIENCE

We accept this thesis as conforming  
to the required standard

.....*R. Karporella*.....  
.....  
.....  
.....

THE UNIVERSITY OF BRITISH COLUMBIA

APRIL 1991

(c) IAN PILKINGTON , 1991

**ABSTRACT**

Two insitu measuring techniques which utilize the seismic piezocone were conducted at three sites to determine the anisotropic stress conditions at each site. The downhole seismic method produced a shear wave velocity profile that is related to anisotropic stress conditions. The crosshole seismic method produced two velocity profiles, one related to anisotropic stress conditions, and the other related to isotropic stress conditions. Ratios of the anisotropic velocities to the isotropic velocities were made and plotted versus depth. These profiles were then compared to determine if anisotropic stress conditions could be evaluated from the plots, and if an estimation of  $K_0$  for the soil could be made. The results obtained at three research sites are included and discussed.

**ACKNOWLEDGEMENTS**

I would like to thank Dr. R.G. Campanella for providing me with the summer job that led to this interesting and challenging thesis topic.

I would also like to thank John Sully for tutoring me through the technical, organizing and revising of this thesis.

To my girlfriend Barbara, for not getting frustrated with me all those weekends I had to spend working on this thesis.

And lastly, to my father, whose moral and financial support has allowed me to achieve an education that may not have been possible otherwise.

## TABLE OF CONTENTS

Abstract	ii
Acknowledgments	iii
List of Figures	v
Chapter 1 - Introduction	1
Chapter 2 - Procedures and Equipment	5
2.1 - Equipment	5
2.2 - Procedure	11
2.2.1 - Downhole Seismic Method	11
2.2.2 - Crosshole Seismic Method	15
Chapter 3 - Theory	19
3.1 - Calculation of Velocities	19
3.1.1 - Cross-over Point Method	20
3.1.2 - Cross-correlation Method	23
3.2 - Comparison of Seismic Velocities	26
Chapter 4 - Site Descriptions	29
4.1 - Laing Bridge South Site	29
4.2 - 232nd St. Site, Langley	29
4.3 - 200th St. Site, Langley	30
Chapter 5 - Test Results	31
5.1 - Laing Bridge South Site	31
5.1.1 - Downhole Seismic Profile	31
5.1.2 - Crosshole Seismic Profile	31
5.1.2a - HV Shear Wave Velocities	31
5.1.2b - HH Shear Wave Velocities	35
5.1.3 - Comparison of Velocity Ratios	36
5.1.4 - Plot of $K_0$ with Depth	38
5.2 - 200th St. Site	40
5.2.1 - Downhole Seismic Profile	40
5.2.2 - Crosshole Seismic Profile	44
5.2.2a - HV Shear Wave Velocities	44
5.2.2b - HH Shear Wave Velocities	47
5.2.3 - Comparison of Velocity Ratios	47
5.2.4 - Plot of $K_0$ With Depth	50
5.3 - 232nd St. Site	52
5.3.1 - Downhole Seismic Profile	53
5.3.2 - Crosshole Seismic Profile	55
5.3.3 - Comparison of Velocity Ratios	56
5.3.4 - Plot of $K_0$ With Depth	58
Chapter 6 - Conclusions	60
References	62
Appedicies	64

## LIST OF FIGURES

Fig 1 - U.B.C. seismic piezocone (receiver cone)	6
Fig 2 - U.B.C. vane cone (source cone)	6
Fig 3 - Photo of the U.B.C. insitu truck	8
Fig 4 - Photo of the cone pushing trailer	8
Fig 5 - Photo of hammer / tripod apparatus	10
Fig 6 - Diagram of downhole seismic arrangement	12
Fig 7 - Diagram of a VH wave	14
Fig 8 - Diagram of crosshole seismic arrangement	16
Fig 9 - Photo of anvil head for source cone rods	18
Fig 10 - Diagram showing the cross-over method	21
Fig 11 - Diagram showing the cross-correlation method	25
Fig 12 a-f - Vel vs depth plots for Laing Bridge	32 - 34
Fig 13 a,b - Vel ratio vs depth plots, Laing Bridge	37
Fig 14 a,b - Profile of $K_0$ vs depth, Laing Bridge	39
Fig 15 a-f - Vel vs depth plots for 200th St.	41 - 43
Fig 16 - Crosshole seismic signal showing two peaks	45
Fig 17 a,b - Vel ratio vs depth plots, 200th St.	49
Fig 18 a,b - Profile of $K_0$ vs depth, 200th St.	51
Fig 19 a,b - Vel vs depth plots for 232nd St.	54
Fig 20 a,b - Vel ratio vs depth plots, 232nd St.	57
Fig 21 a,b - Profile of $K_0$ vs depth, 232nd St.	59

## CHAPTER ONE

### INTRODUCTION

Insitu soil testing has developed from a research tool into a viable and competent source of obtaining soil parameters. Used in conjunction with, or even at times as a substitute for traditional soil testing procedures, such as the standard penetration test (SPT), soil tube sampling, and test pits, cone penetration testing can provide a more continuous soil profile with data that are often a better representation of the soil conditions being tested. Also, some insitu methods obtain data that can be utilized to calculate parameters not easily found using traditional sampling procedures. One such technique is the crosshole seismic velocity method, which has been performed in the past by Stokoe and Woods (1972).

In the crosshole seismic velocity method, two cone penetration test (CPT) units are used for the source and the receiver. The receiver cone is actually a seismic piezocone that has an accelerometer installed in it's body. Generation of a seismic shear wave in the source cone is done by hitting the cone rods at the surface. The shear wave travels to the

receiver cone, where the accelerometer picks up the wave signal and the time for the wave to travel between the two cones is recorded. The travel time of a seismic wave reflects the characteristics of the soil between the two units. If such travel times are measured at certain depth intervals as the cones are pushed deeper into the soil, a profile can be developed of travel times with depth. Knowing these travel times, as well as the distance between the source and the receiver, the change in seismic velocities with depth can be calculated.

The seismic velocities measured in a soil layer can be related to the stress conditions of the soil by the equation:

$$V_s = C \sigma'^n$$

Where

$V_s$  = shear wave velocity

$\sigma'$  = effective stress of the soil

C and n = constants related to the soil properties

It has been proposed that  $V_s$  is dependent on the direction the shear wave is travelling in, as well as the direction of particle motion caused by the shear wave (Roessler 1979).

Therefore, if shear waves are generated with particle motion in the vertical and horizontal direction, the stress conditions in the vertical and horizontal plane can be compared to show the effects of anisotropy in the soil. Anisotropy in a soil can occur from two possibilities; structural conditions, and stress conditions. Structural anisotropy is due to layers of soil with different physical characteristics (density, mineralogy, etc.). Stress anisotropy is due to different stress conditions in the vertical and horizontal plane. If the soil stratigraphy in the area being tested is known to be uniform, then structural anisotropy can be ignored, and the shear wave velocities will relate to stress anisotropy.

Shear wave velocities are also related to another soil parameter, the small - strain shear modulus, by the equation:

$$G_o = \rho V_s^2$$

Where

$G_0$  = shear strain modulus

$\rho$  = bulk density of the soil

Therefore, a knowledge of the seismic shear wave velocity profile with depth will give a profile of  $G_0$  with depth as well.

Lastly, ratios of the velocities generated with particle motion in the vertical and horizontal plane can be related to  $K_0$  through various equations which are discussed in detail by Lee and Stokoe (1985).

The objective of this thesis is to determine whether seismic shear wave velocities generated in the vertical and horizontal plane can be compared to show a profile of the stress conditions in the soil.

CHAPTER TWO  
PROCEDURES AND EQUIPMENT

**2.1 - EQUIPMENT**

To obtain a detailed soil profile, three CPT cones were utilized in this technique. The two receiver cones were UBC cone 7 and UBC cone 8, which are standard 10 cm<sup>2</sup> cross sectional area piezocones built by UBC technicians, equipped with pore pressure transducers and seismic accelerometers within the cone body (Fig. 1). The source cone was also constructed at UBC's Civil Engineering machine shop. It is a 15 cm<sup>2</sup> cross sectional area cone with twelve vanes machined into the body (Fig. 2). This cone also had bender elements installed to act as a trigger for denoting when the seismic waves were initially generated, but it was later deemed unnecessary and were subsequently removed.

One of the receiver cones was pushed into the ground using the UBC Civil Engineering Insitu Soil Testing truck. This vehicle consists of a Ford LN 600 one ton truck with a power take off connected to a hydraulic pump and a custom made box mounted on the frame. The interior of this box is equipped with

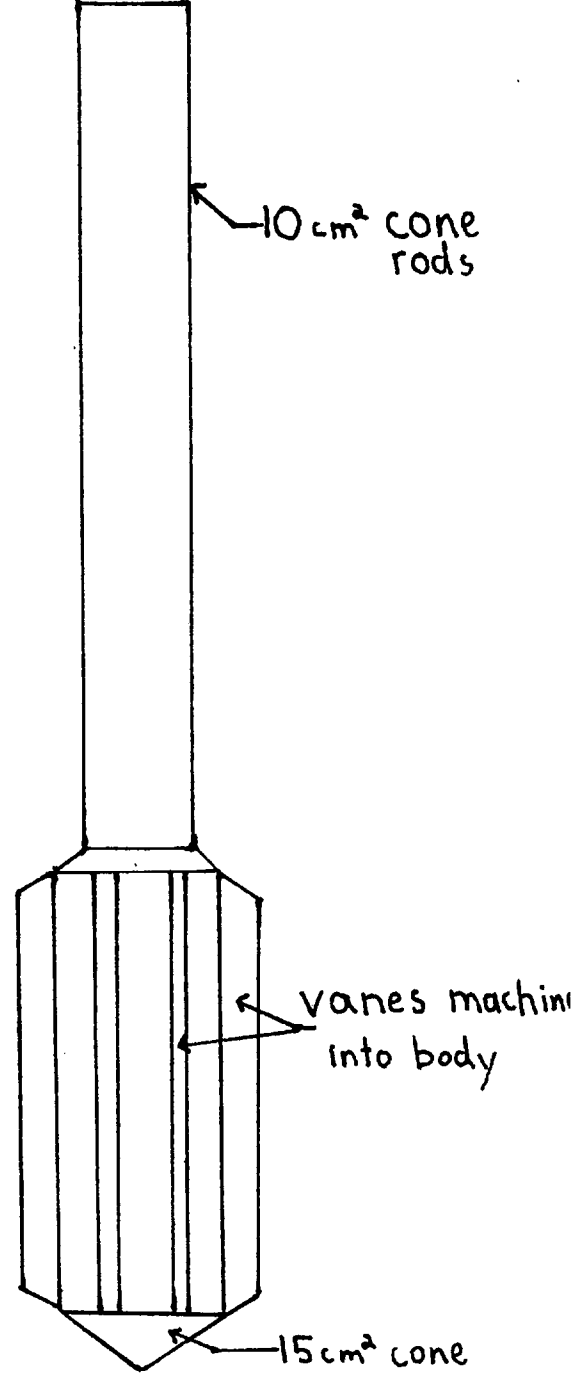
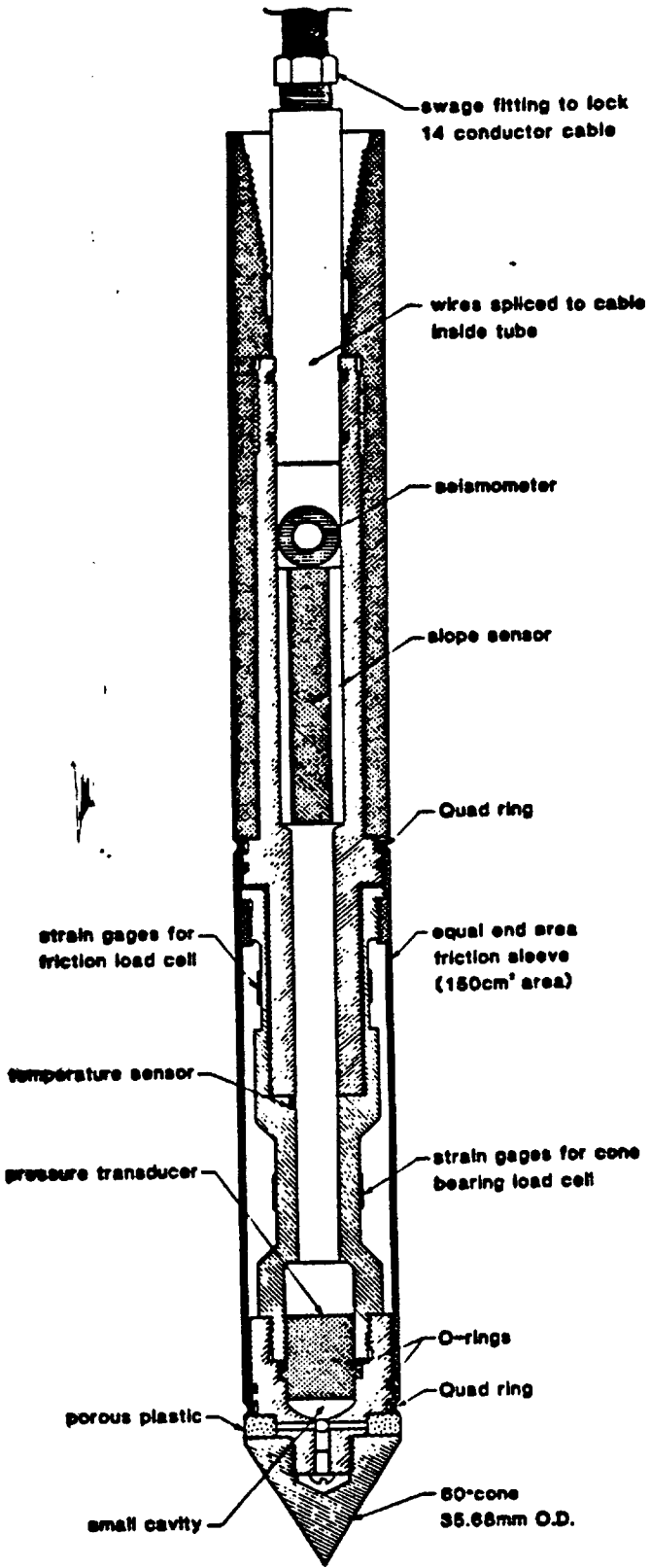
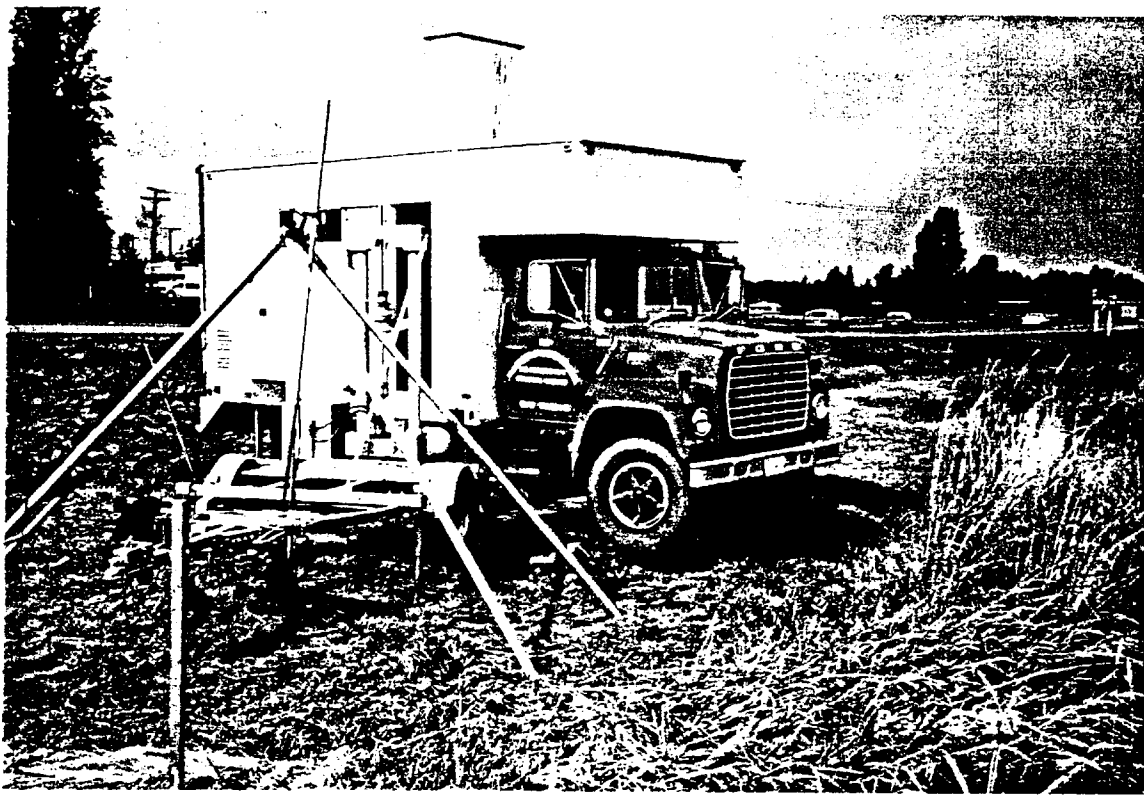


Fig 1 - UBC seismic piezocone (receiver cone) (from Campanella 1990)

Fig 2 - UBC vane cone (source cone)

a hydraulic pushing ram capable of applying over 10 tons of downward force. The ram houses a machined head that enables various types of probes to be pushed down and also retrieved back out of the ground. The box is also equipped with various electronic data collection equipment for the numerous probes used in the department. With the vehicle configured this way, the receiver cone was easily pushed into the ground and the recording of the data was done in a comfortable enclosed environment (Fig. 3).

The second of the two receiver cones was pushed into the ground using a trailer that was designed, and assembled in the Civil Engineering machine shop. The lightweight boat trailer frame has a retractable mast that utilizes a hydraulically driven pushing head. Hydraulic power is obtained from external hydraulic lines plugged into the Insitu Soil Testing truck's main hydraulic system (Fig. 4). This design kept the trailer simple and lightweight, allowing two people to easily manoeuvre the trailer by hand into the desired location. However, the downfall of such a light rig is the lack of weight to counteract the high pushing forces emplaced on the cone as it is being driven into the ground. To compensate for this, earth anchors



8

Fig 3 - Photo of the insitu truck with the cone pushing trailer and hammer tripod in the foreground

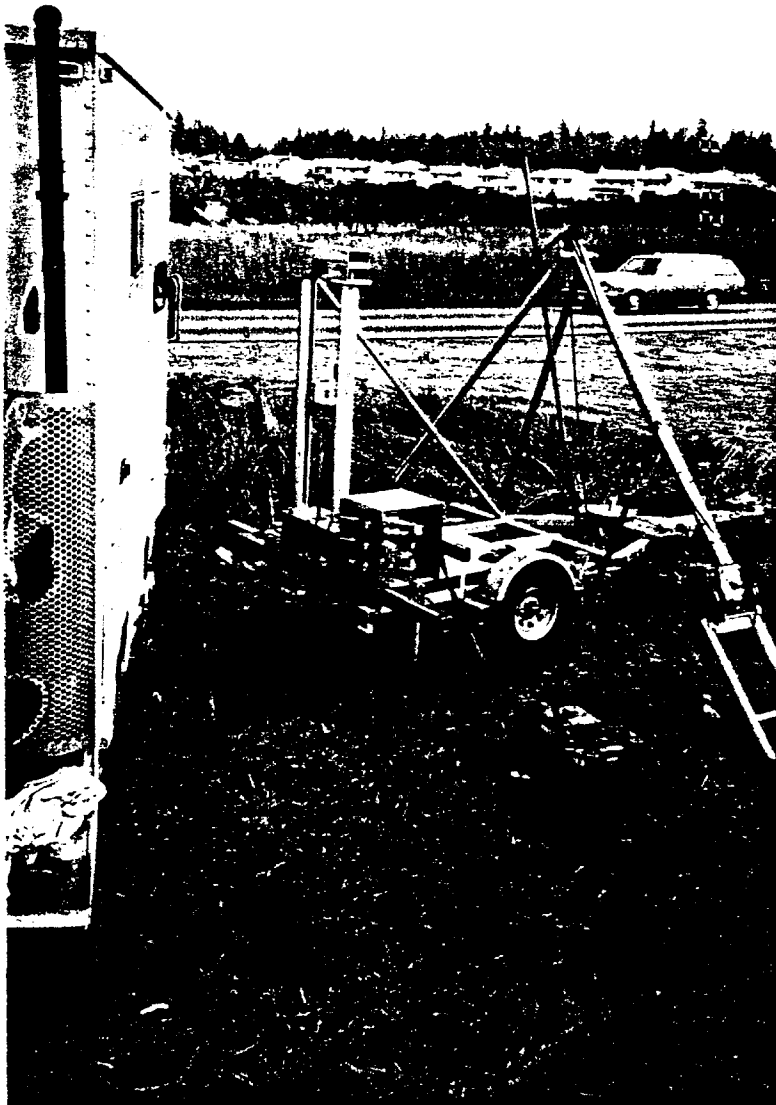


Fig 4 - Photo of cone pushing trailer

are hydraulically augured into the ground and attached to the trailer.

The source cone (vane cone) was pushed into the ground using a different technique. Since there were no fragile electronic parts within the cone body (except for the bender elements, which were later removed), the source cone was driven into the ground using a portable tripod with a hammer system on loan from Klohn Leonoff (Fig 5). This apparatus consists of a lightweight aluminum tripod. A fifty pound hammer, which slides on a steel shaft mounted on top of the cone rods, is positioned in the centre of the tripod. A rope attached to the hammer runs up through the middle of the tripod, around a pulley at the top and down one of the tripod legs to a small portable motor with a cathead pulley attached. By winding the rope around the cathead and increasing the tension by pulling on the rope, a mechanical advantage can be achieved to allow an operator to easily lift the hammer with one hand. By repeatedly lifting and dropping the hammer on the cone rods attached to the cone, the cone can be driven into the ground much like a pile driver.

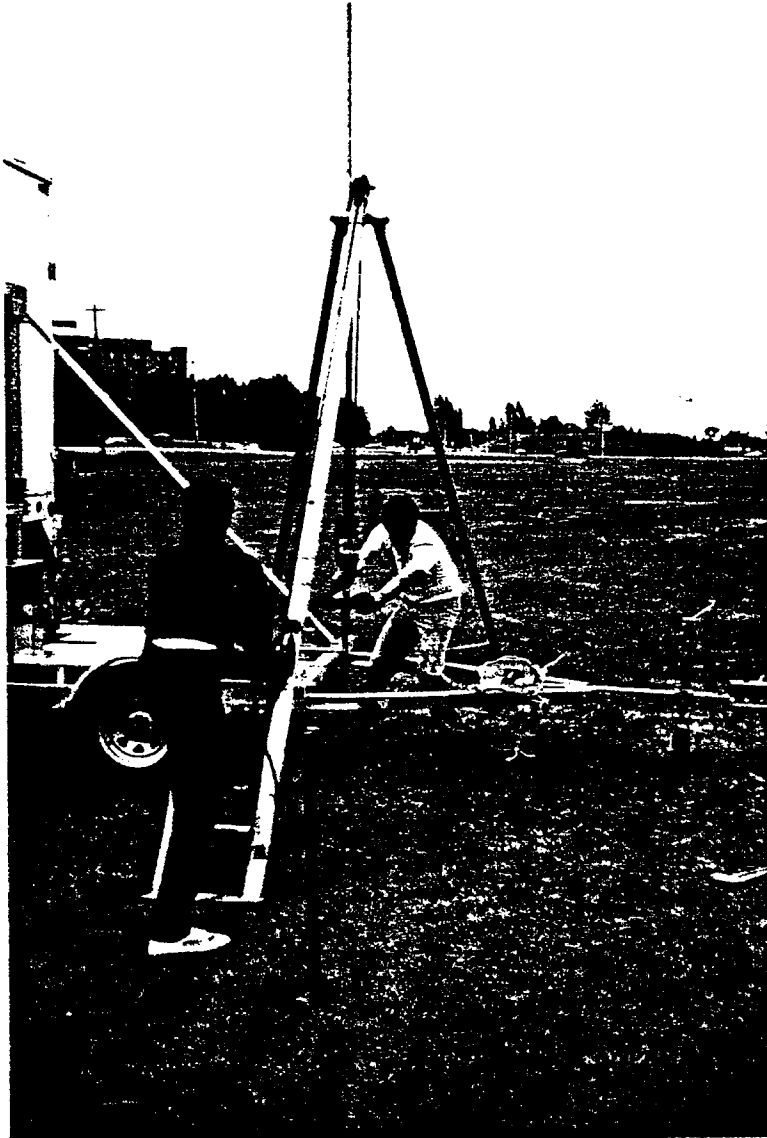


Fig 5 - Photo of hammer / tripod apparatus

Due to the low reaction force of this light weight apparatus, the tripod is assisted by the Insitu truck, which pushes a 10 cm<sup>2</sup> dummy cone down to the required depth of investigation to open a hole for the source cone. Since the source cone is 15 cm<sup>2</sup> in cross sectional area, not including the vanes, the cone vanes are still in solid contact with soil when it is driven into the ground, but the tripod will be able to penetrate the cone by driving with little trouble.

## **2.2 - PROCEDURE**

Two different techniques were used in the acquisition of the travel times of the seismic waves, the downhole seismic method and the crosshole seismic method.

### **2.2.1 - DOWNHOLE SEISMIC METHOD**

The downhole seismic method involves pushing the piezocone into the ground using the Insitu truck, and stopping at certain intervals, in our case either half-metre or one metre intervals. At each of these intervals, a seismic wave is generated by hitting a sledge hammer on the front footing pad that elevates and levels the truck off the ground (Fig. 6). This is done on

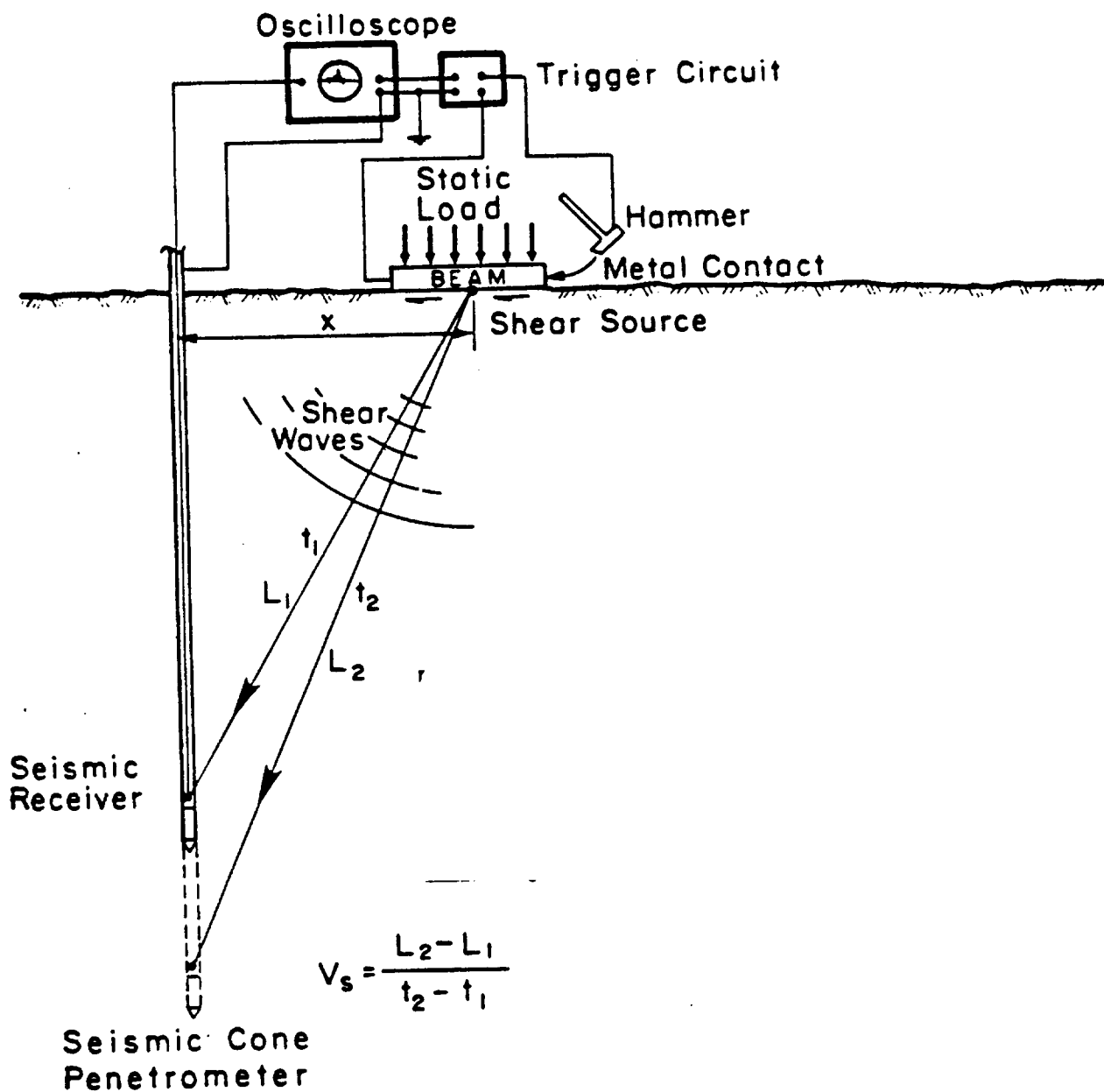


Fig 6 - Diagram of downhole seismic arrangement

(from Campanella and Stewart 1990)

both the left and right sides of the front pad of the truck. The sledge hammer is wired to a trigger box. The trigger box and the accelerometer in the cone are connected to a Nicolet oscilloscope recorder. When the hammer hits the truck pad it grounds out, starting the oscilloscope timer at the same time the seismic shear wave is generated. When the seismic shear wave reaches the accelerometer in the cone, the oscilloscope records the waveform. This waveform can be stored on a 5 1/4" floppy disk for later processing. Knowing the depth of the cone, distance of the hammer horizontally from the cone hole and using a little trigonometry, the seismic velocity of the wave can be calculated (Fig. 6)

Seismic shear waves generated in this manner have a unique geometry. The shear wave travels vertically towards the receiver cone, but the particle motion of the soil is in the horizontal plane. In an attempt to keep the geometries of the different seismic shear waves comprehensible, a simple notation system will be adopted, in which V indicates the vertical plane, and H indicates the horizontal plane. Therefore, a downhole generated seismic velocity is labelled a VH wave. This wave is shown graphically in Figure 7.

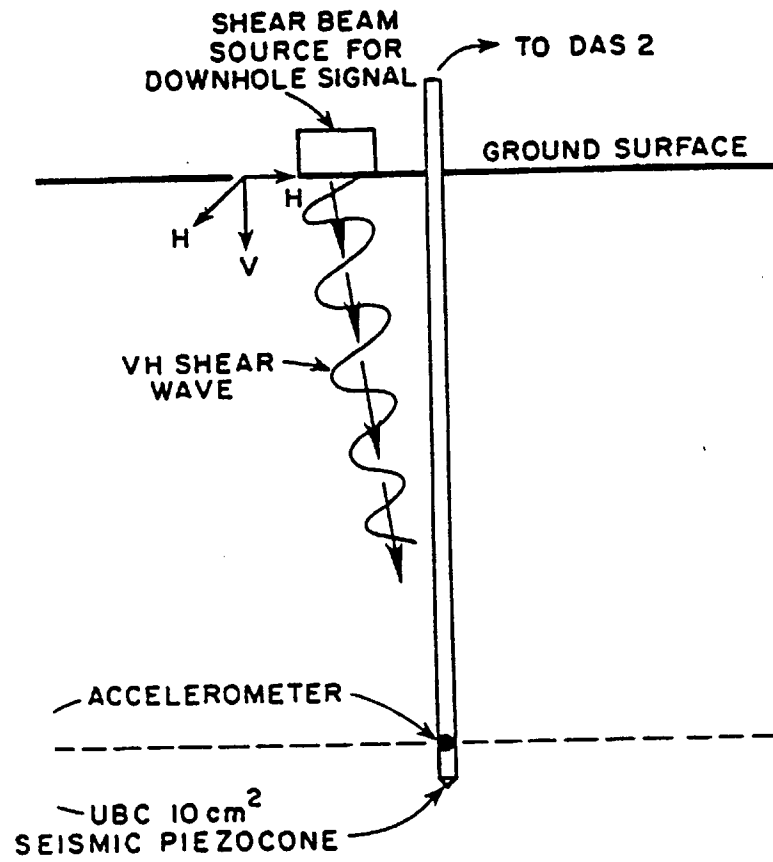


Fig 7 - Diagram of downhole seismic setup showing a VH wave  
(from Sully 1991)

The down hole seismic technique has been utilized in previous research projects (Campanella and Robertson 1984) and is a proven method of obtaining a seismic velocity profile with depth.

#### **2.2.2 - CROSSHOLE SEISMIC METHOD**

The crosshole seismic method also has been used in the field, but we are taking the technique one step further. Our technique has never been attempted in the field, but it has been simulated in a lab (Lee and Stokoe 1985, and Yan and Byrne 1989). This technique utilizes the source vane cone and all the other apparatus described in section 2.1. All three cones are driven into the ground and are again stopped at either half-metre or one metre intervals. It should be noted that all three cones are at the same depth, and that the cones are aligned in as straight a line as possible, with the source cone at one end of the line (Fig. 8). The reasoning behind using two receiver cones in this technique will be discussed later in Chapter Three. An anvil head mounted on top of the source cone rods had two arms that allowed the generation of four wave types.

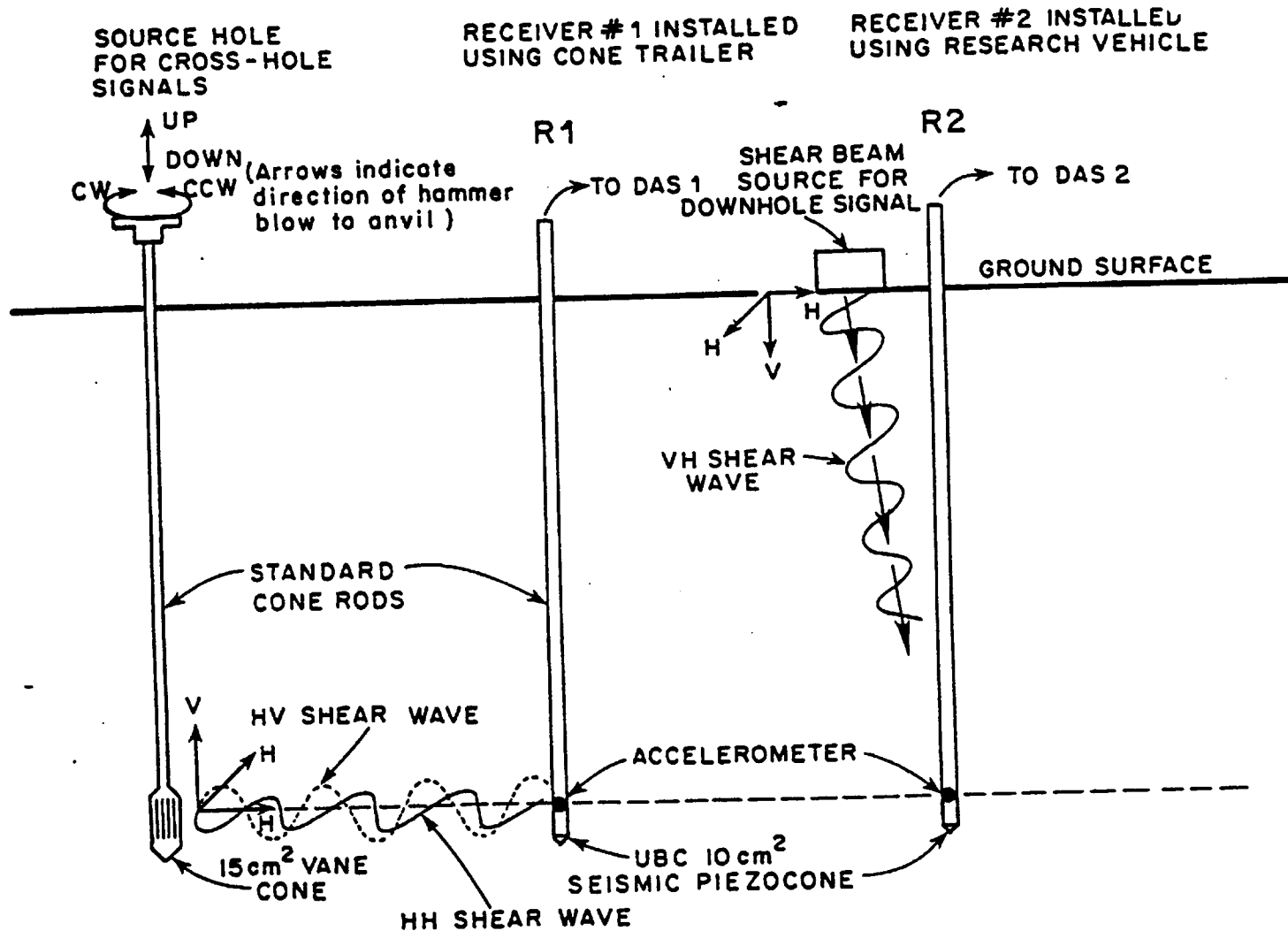


Fig 8 - Diagram of the crosshole seismic arrangement  
(from Sully 1991)

The head could be hit vertically up and down, and also hit in a torsional manner clockwise and counterclockwise (Fig. 8). Using the same notation system as the downhole seismic method, the four waveforms generated are two HV waves (vertical up / down hits) and two HH waves (torsional clock / counterclockwise hits). A photo of the anvil head can be seen in Figure 9.

Again, the hammer is connected to the trigger box and the two receiver cones are connected to the Nicolet oscilloscope for recording of the four wave forms generated.

Originally, the source cone had bender elements installed within the cone body. These elements were to act as an accelerometer to detect when the seismic shear wave was generated. It was originally assumed that there would be a delay between when the cone rods were hit at the surface (which started the oscilloscope), and when the seismic shear wave would be generated in the soil. However, it was found that the generation of the seismic shear wave was almost instantaneous after hitting the cone rods, and therefore the bender elements were deemed unnecessary and removed.



Fig 9 - Photo of anvil head for the source cone rods

## CHAPTER THREE

### THEORY

#### **3.1 - CALCULATION OF VELOCITIES**

The data obtained in the field were recorded as waveforms as seen in the oscilloscope. To observe the data more conveniently and calculate the arrival times of the seismic waves, a soft-ware program called VU-POINT™ was utilized. This program allows one to view a waveform either in the time domain (graph of voltage vs. time) or in the frequency domain (graph of voltage vs. frequency). It also allows two or more graphs to be put on the screen at once for comparison purposes. This program also has many other powerful functions, such as performing Fast-Fourier transforms on waveforms, filtering unwanted signals, and a host of other features that will not be discussed here. This program can be conveniently used on an IBM compatible.

Two techniques were used in the calculation of the arrival times of the seismic waves so each technique would double-check the other. One method is called the cross-over point method, while the other is called the cross-correlation method.

### 3.1.1 - CROSS-OVER POINT METHOD

In the cross-over point method, the arrival time is determined by noting on the voltage vs. time graph when the first wave arrives. However, it is sometimes hard to determine which wave crest is the actual first arrival of the seismic wave, due to electrical noise or a less than clean signal. To eliminate this problem, we overlay the signal that was generated in the opposing direction; ie. for the downhole technique we overlay the signal generations from the left and right side of the truck at the same depth. For the crosshole technique we overlay the up and down hits made on the head, and the left and right (clockwise and counterclockwise) hits on the head. On the voltage vs. time graph of these overlays, it can be seen that the opposing hit has an almost identical signal, but it is the mirror image of the first signal (Fig 10). Therefore, consistent arrival times can be obtained if the first cross-over point is used as a marker. As the cone is moved to greater depths, the cross-over point of a signal occurs at a later time due to the greater distance of the cone from the source. Noting the difference in time  $\Delta t$  between two depth intervals

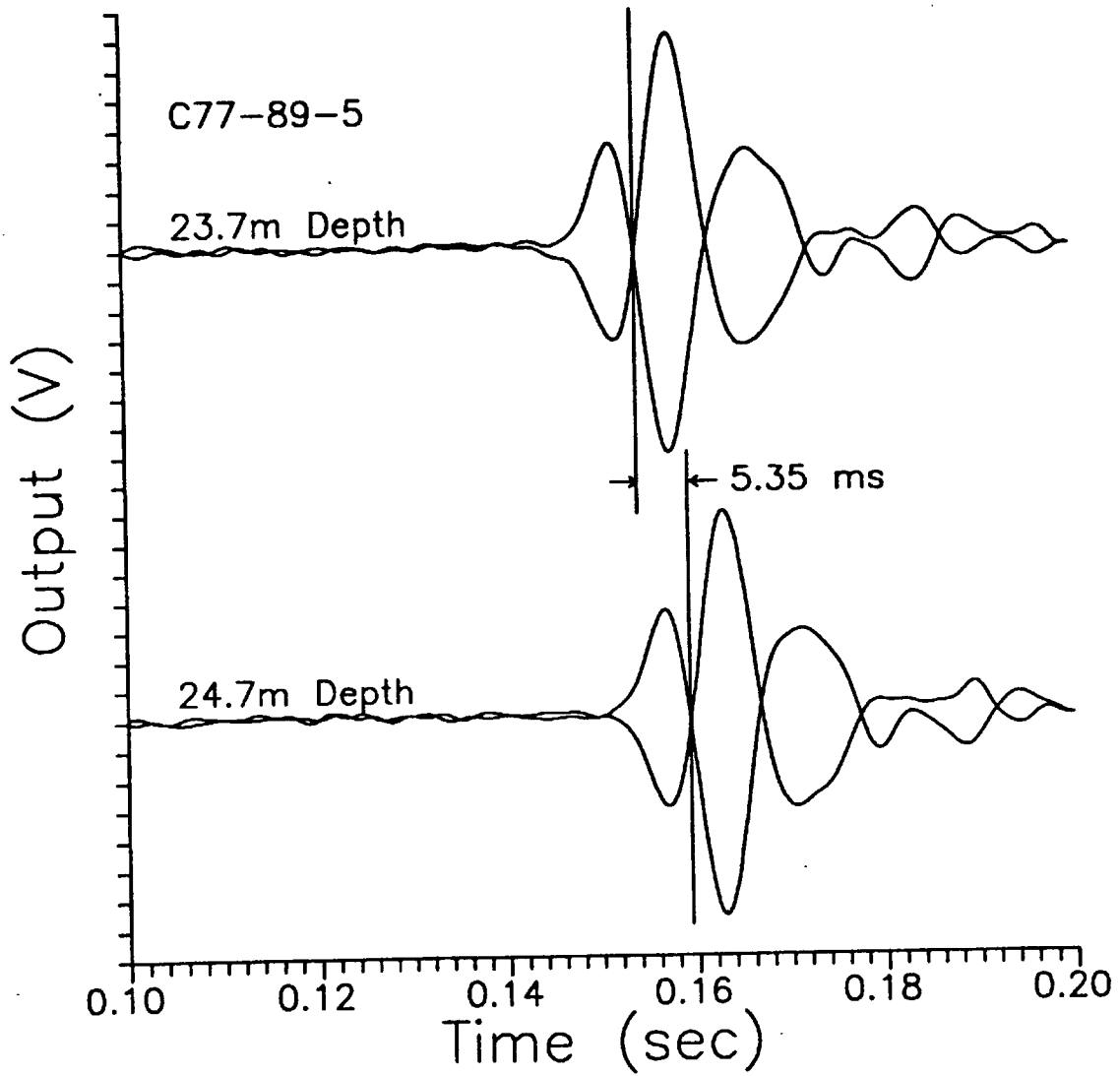


Fig 10 - Diagram showing the cross-over method  
for a time arrival

(from Campanella and Stewart 1990)

(in Fig. 10,  $\Delta t = 5.35$  ms) a simple equation can be used to calculate the velocity:

$$\text{Velocity} = \frac{L_2 - L_1}{\Delta t}$$

Where  $L_1$  and  $L_2$  are defined in Figure 6.

In the crosshole seismic method, this same principal is used. However, since the arrival times are being measured in a horizontal plane (unlike the downhole seismic method, which measures arrival times in a vertical plane), a difference in travel times between two depth intervals is not possible. Therefore, two receiver cones are utilized, one a greater distance from the source than the other (Fig. 8). The arrival times to each cone is measured, and the difference in these two times,  $\Delta t$  is measured. The horizontal distance from the source to each cone is determined,  $X_1$  and  $X_2$  and the velocity between these cones is calculated from the equation;

$$\text{Velocity} = \frac{X_2 - X_1}{\Delta t}$$

Note that in this case, the difference  $X_2 - X_1$  is constant at every depth interval, unlike the downhole seismic method, where  $L_1$  and  $L_2$  are continuously increasing.

To make the data more presentable and easier for comparison purposes, the data are usually plotted as a velocity vs. depth graph.

### 3.1.2 - CROSS-CORRELATION METHOD

The second method used to calculate arrival times of the seismic waves is called the cross-correlation method. This method is conceptually more complicated and difficult to explain, so a simplified description of the method will be given here. For an in depth description of this technique, refer to the paper Seismic Cone Analysis Using Digital Signal Processing for Dynamic Site Characterization by R.G. Campanella and W.P. Stewart (1990).

In this method, a comparison is made between two waveform signals at different depth intervals (in the downhole technique), or between the two receiver cones (in the crosshole technique). The signals compared are the same type of signal; ie. In the downhole technique, a comparison of the left side hit

wave generations at 1m and 2m depth is done. The signal from the receiver that is farther away from the source will have a later arrival time than the closer receiver signal. The more distant signal is shifted relative to the closer signal in time increments and the two waveforms are compared. This step is repeated until the two wave forms are matched. The time shift that was required to produce this match is the time difference between the two receivers (Fig.11). It should be noted that this technique was described in the time domain for ease in describing the concept. However, it is very time consuming for a PC using VU-POINT to perform this calculation, a typical calculation taking about 10 minutes on a 386 PC. To speed up this process, the waveform is converted to the frequency domain for calculation purposes, and the results are converted back to the time domain to obtain the time difference. Again this procedure is described in more detail in Campanella and Stewart (1990). The calculated time difference is then used to find the seismic wave velocity for this interval using the equations utilized in the crossover method. This data is again plotted on a velocity vs. depth graph for comparison purposes.

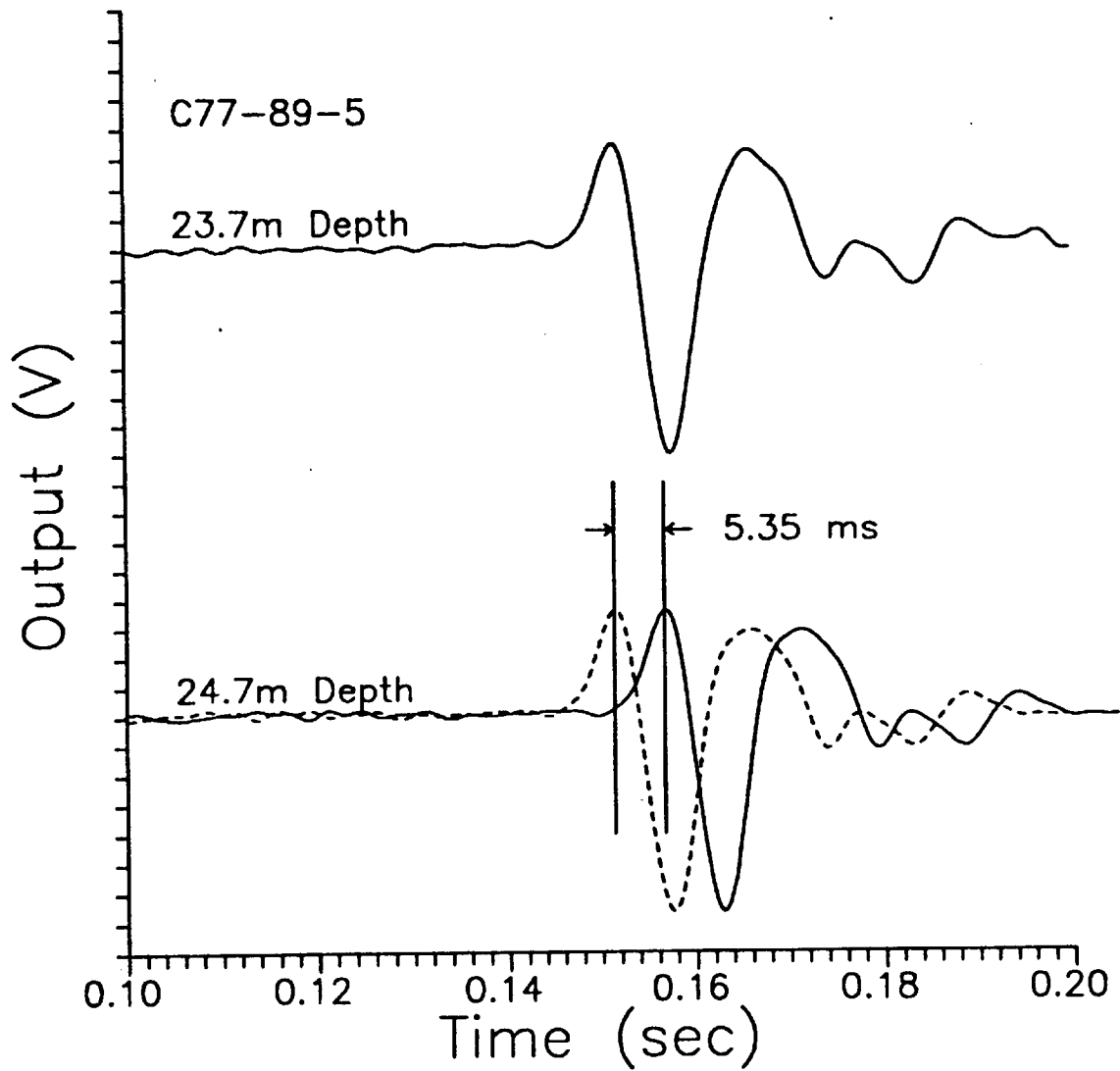


Fig 11 - Diagram showing the cross-correlation method  
for a time interval

(from Campanella and Stewart 1990)

Macros developed by Stewart (1991) for use with the VU-POINT program were used for all cross-correlation wave velocity determinations.

### 3.2 - COMPARISON OF SEISMIC VELOCITIES

The three wave generation techniques described in Chapter Two (downhole seismic and two types of crosshole seismic) produce waves that are different in either wave direction or particle motion. The stress conditions in the plane of wave direction and the plane that particle motion occurs in will be reflected in the shear wave velocity by the equation:

$$V_s = C \sigma'^n$$

The equation above can be expanded to relate directly to either the anisotropic stress conditions or the isotropic stress conditions. The downhole seismic wave velocities (VH waves) and the HV waves from the crosshole seismic method will give velocities that relate to the anisotropic stress. These are termed  $(V_s)_A$ , with the related stresses being  $\sigma'_v$  and  $\sigma'_h$ . The HH waves from the crosshole seismic method will give velocities that are related to the isotropic stress. These are termed

$(V_s)_I$ , with the related stress being  $\sigma'_h$ . The expanded equations that are related to the two stress conditions are discussed in detail by Sully (1991). These equations can then be rearranged in terms of  $K_o$ , the lateral stress parameter, where:

$$K_o = \frac{\sigma'_h}{\sigma'_v}$$

A summary of the rearranged equations is given as:

$$\frac{(V_s)_A}{(V_s)_I} = \frac{C_D}{C_C} \left( \frac{1 + K_o}{2K_o} \right)^{nt}$$

$$\frac{(V_s)_A}{(V_s)_I} = \frac{C_D}{C_C} \frac{1}{K_o^{na}}$$

Where  $C_D$  and  $C_C$  are directional stiffness constants. The first equation is determined from a technique called the average stress method, while the second equation is developed from the individual stress method (Sully 1991). To determine absolute values from these equations, the constants  $C_D$ ,  $C_C$ ,  $nt$ , and  $na$  have to be determined, which is not an easy task. However, from previous research references, a  $C_D / C_C$  ratio of 1, an  $nt$  value of 0.25, and an  $na$  value of 0.125 was decided upon for use in

the above equations to determine  $K_0$  (Sully 1991). Graphs of  $K_0$  versus depth were then plotted.

**CHAPTER FOUR**  
**SITE DESCRIPTIONS**

**4.1 - LAING BRIDGE SOUTH SITE**

This site is situated on the eastern point of Sea Island, east of the south on-ramp to the Arthur Laing Bridge. The site is comprised of deltaic deposits that have been eroded and transported by the Fraser River. The general stratigraphy of the site is a 2m thick crust of clay silt at the surface, followed by a 18-20m thick zone of interbedded fine to medium sand with minor silt layers and occasional organic material, followed by a thick zone of interbedded fine sand and clay silt. Our depth of interest is the first 10 metres. The soil is loose to medium dense sand, and the water table fluctuates between 1m and 2m depth below ground level.

**4.2 - 232nd St. SITE, LANGLEY**

This site is located adjacent to the Trans-Canada Highway on the north side, just west of the 232nd St. off-ramp. The site area comprises of the Capilano Sediments, raised marine deltaic deposits. The general stratigraphy of the site consists

of 30+ m of marine silt to clay deposited during glacial regression, with occasional interbedded sand layers. The soil is over consolidated at the surface to about 5m depth. The water table fluctuates seasonally between 1.5m below ground level in the summer, and at ground level in the winter. Laboratory tests (Internal Data Report ISTG-1-90, Campanella et al. 1990) indicate a medium plasticity layer at the surface (PI  $\approx$  40) dropping to a low plasticity index at about 3m (PI  $\approx$  20) and staying relatively uniform with depth.

#### **4.3 - 200th St. SITE, LANGLEY**

This site is located approximately 8 km west of the 232nd St. site. The site is on the north side of the Trans-Canada Highway, just east of the 200th St. off-ramp. The stratigraphy of the site is virtually the same as the 232nd St. site, with comparable plasticity values.

**CHAPTER FIVE****TEST RESULTS****5.1 - LAING BRIDGE SOUTH SITE**

The results of the shear wave velocity calculations can be seen in the velocity vs. depth graphs of figures 12 a-f.

**5.1.1 - DOWNHOLE SEISMIC PROFILE**

Looking at figures 12a and 12b, an essentially linear increase in seismic wave velocity with depth can be seen. The cross-correlation method data (Fig. 12b) appears to have better grouping. Therefore, we will use this data for future comparisons. Since the downhole seismic wave velocities (VH waves) are related to the anisotropic stress conditions ( $\sigma_v'$  and  $\sigma_h'$ ), as stated in Chapter Three, it appears that the anisotropic stress increases linearly with depth.

**5.1.2a - CROSSHOLE SEISMIC PROFILE: HV SHEAR WAVE VELOCITIES**

Looking at the HV shear wave plots with depth (Figs. 12c and 12d), again a slight increase in shear wave velocity with depth can be seen. HV waves are also related to the anisotropic

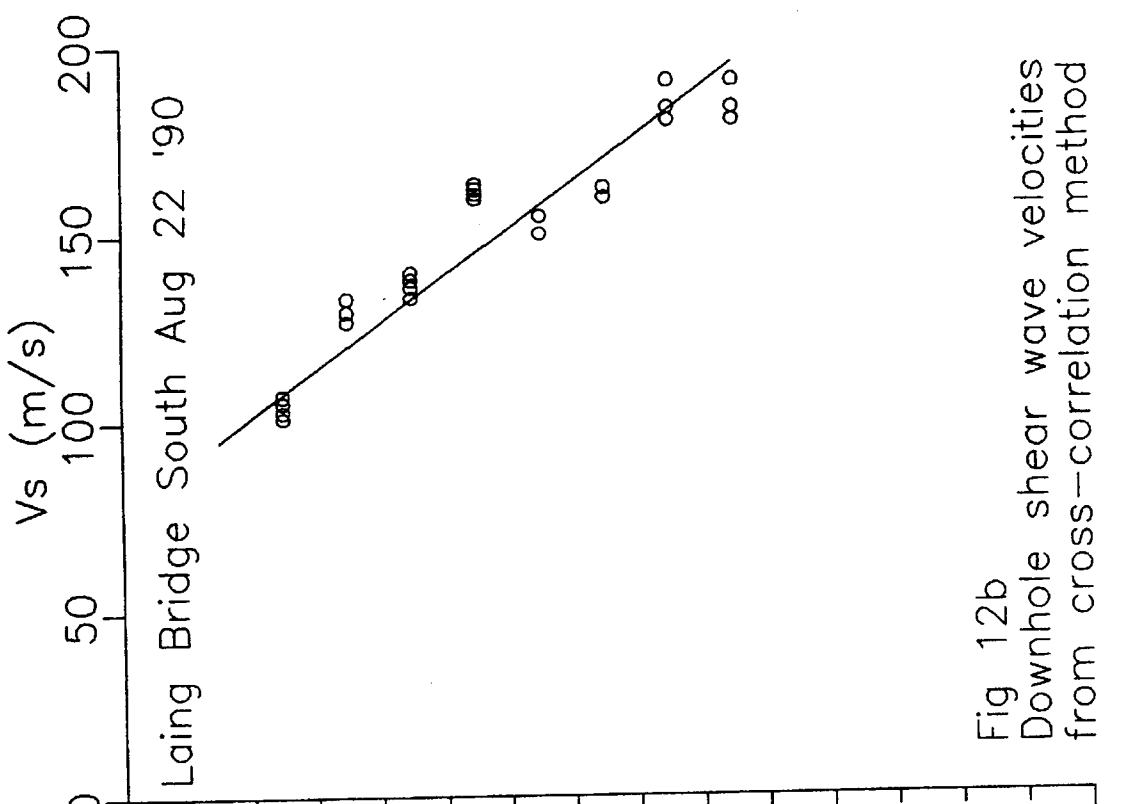


Fig 12b  
Downhole shear wave velocities  
from cross-correlation method



Fig 12a  
Downhole shear wave velocities  
from cross-over point

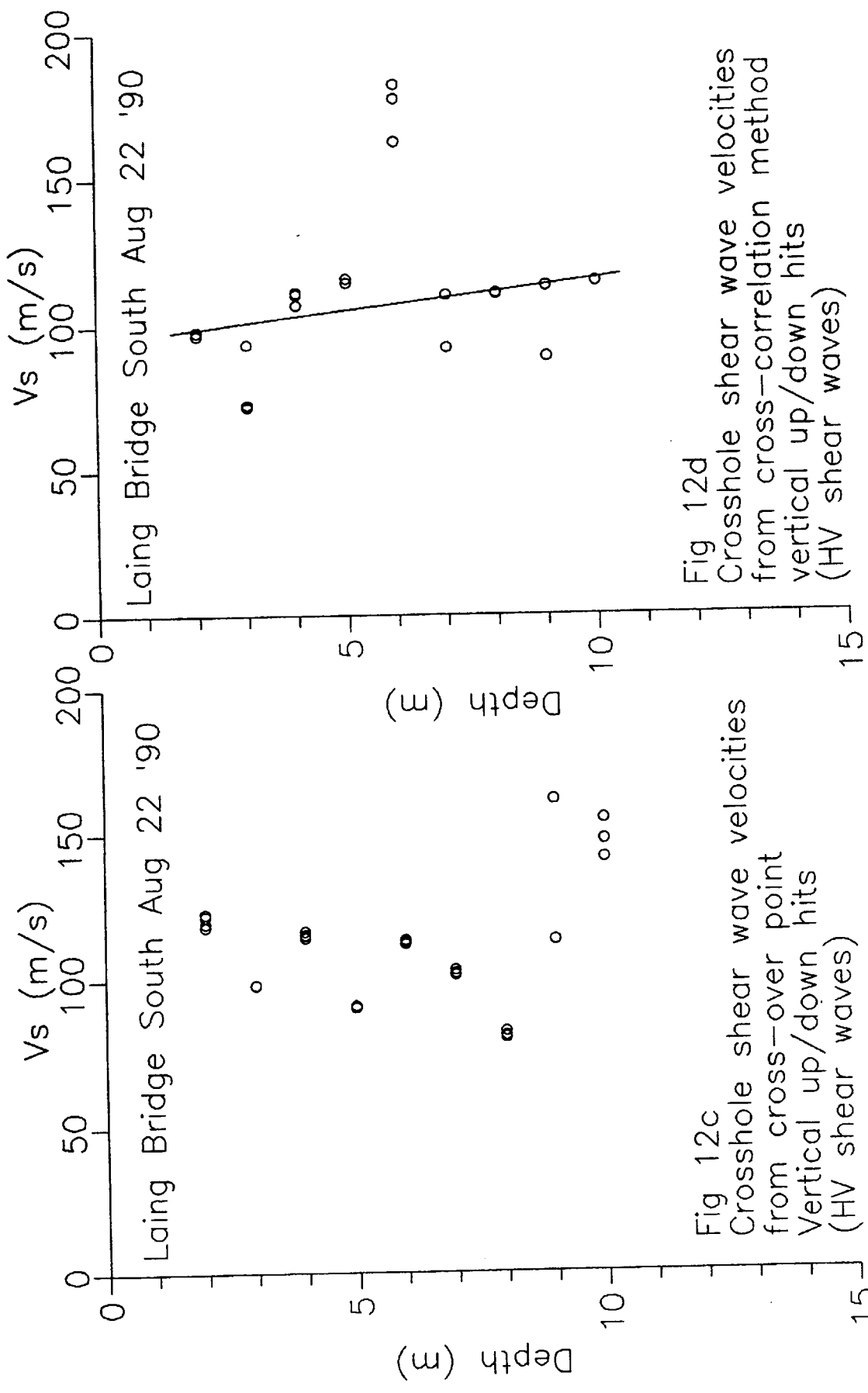


Fig 12c  
 Crosshole shear wave velocities  
 from cross-over point  
 Vertical up/down hits  
 (HV shear waves)

Fig 12d  
 Crosshole shear wave velocities  
 from cross-correlation method  
 vertical up/down hits  
 (HV shear waves)

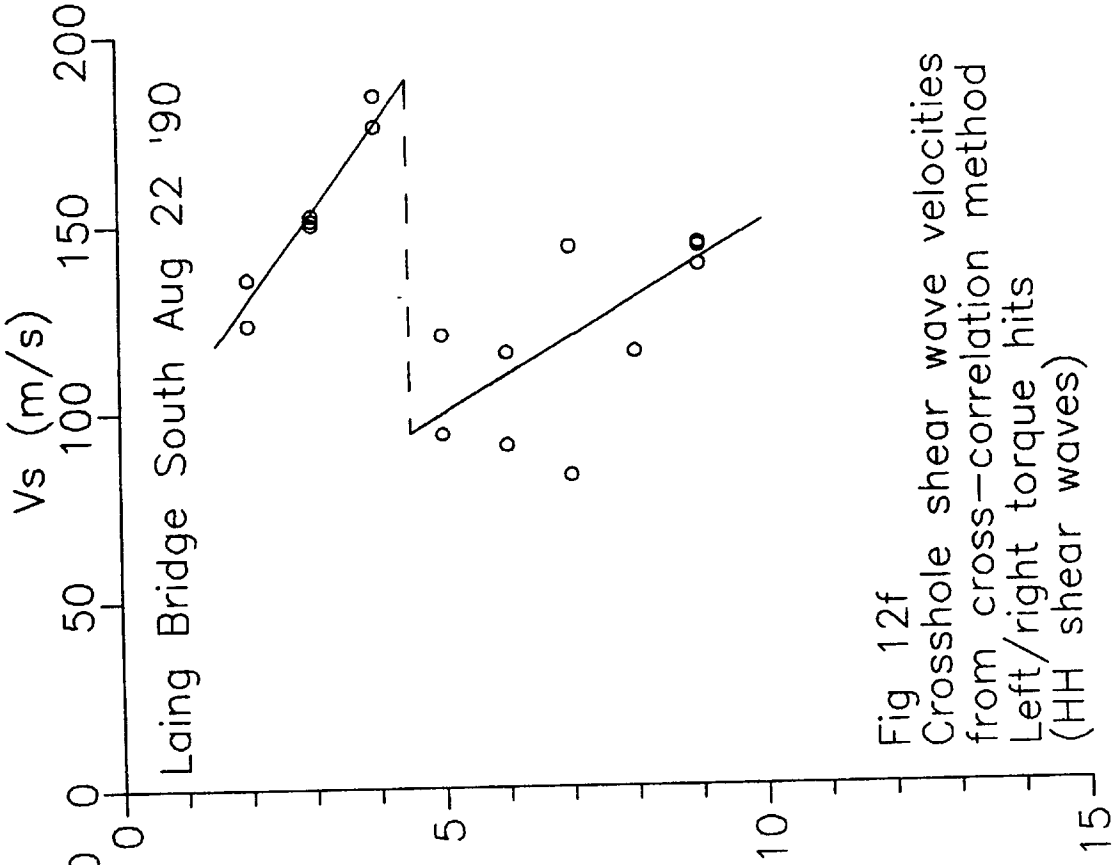


Fig 12f  
Crosshole shear wave velocities  
from cross-correlation method  
Left/right torque hits  
(HH shear waves)

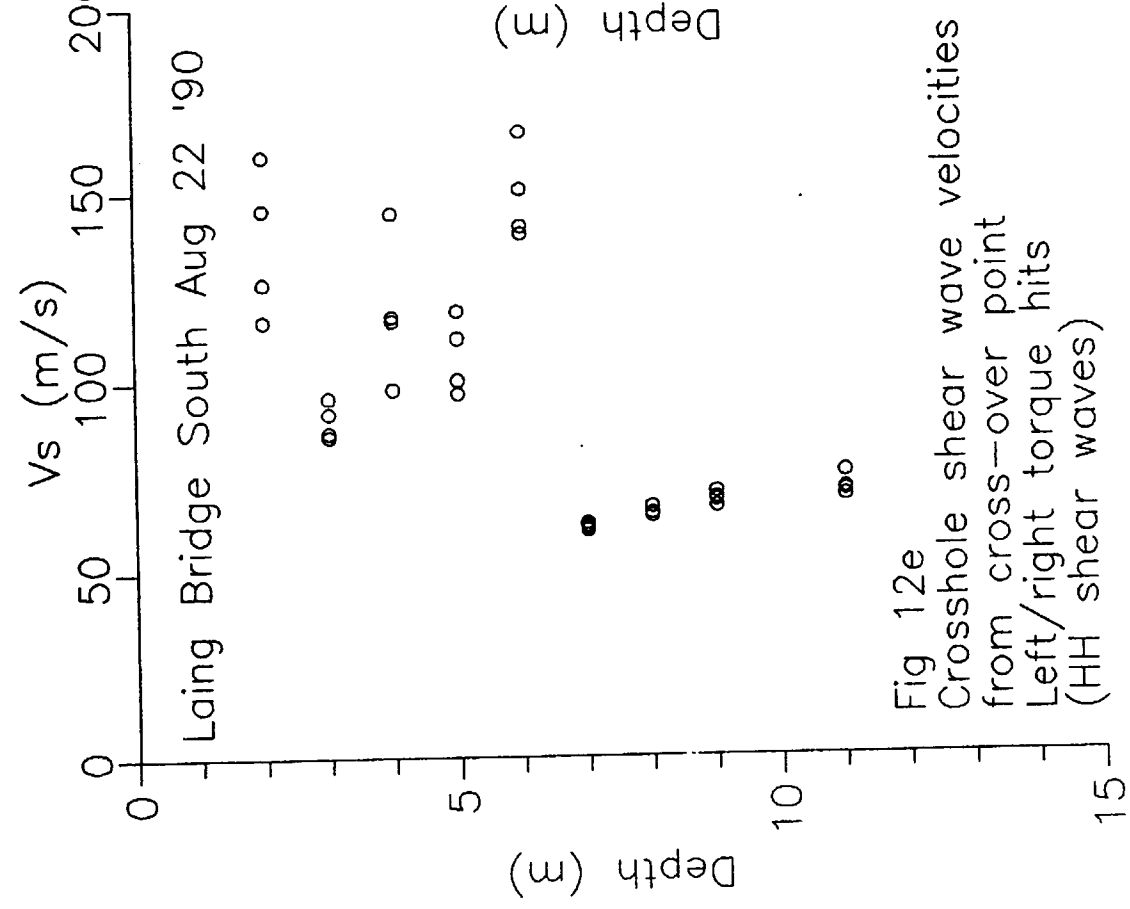


Fig 12e  
Crosshole shear wave velocities  
from cross-over point  
Left/right torque hits  
(HH shear waves)

stress conditions, as stated in Chapter Three. Therefore, a similar trend would be expected between the HV shear wave velocities and the downhole velocities, which is seen here. The cross-correlation data appears to have better grouping once again, and will be used for future comparisons.

#### **5.1.2b - CROSSHOLE SEISMIC PROFILE: HH SHEAR WAVE VELOCITIES**

The HH shear wave plots (Figs. 12e and 12f) seem to have a wide scatter, and the cross-over point data and the cross-correlation data do not coincide well. It has been shown by Campanella et al. (1989) that the cross-correlation method produces more accurate results in sand than the cross-over method. Noting this, and the fact that the cross-correlation data from the downhole seismic and HV shear wave plots are better grouped, the data produced by the cross-correlation data will be used in the discussion of the HH shear wave velocity plot with depth (Fig 12f).

This graph has a wide scatter of data, but it appears to have two distinct linear trends involved. At shallow depths to about 4m, there is a zone of high velocities increasing with depth. Below 5m, the shear wave velocities suddenly drop, and

follow a new trend of linearly increasing with depth. The HH shear waves are related to the isotropic stress conditions, as stated in Chapter Three. Therefore, the linearly increasing trend suggests that the isotropic stress ( $\sigma_h'$ ) is increasing linearly with depth. However, the sudden change in velocities at 5m depth may be due to two physically different soil characteristics, such as a hard crust at the surface contributing to higher velocities, and a loose sand layer below 5m, causing the lower velocities. If this is true, then the HH shear waves are also related to a structural anisotropy in the soil in this case.

### 5.1.3 - COMPARISON OF VELOCITY RATIOS

Figures 13a and 13b show the two anisotropic shear wave velocities related to the isotropic shear wave velocities. Both figures indicate a linearly increasing trend with depth. This suggests that the soil stiffness is increasing with depth. A slight jump in the velocity ratios can be seen at 5m depth. This again may be due to a change in the material properties of the soil, as indicated in the previous sub-section.

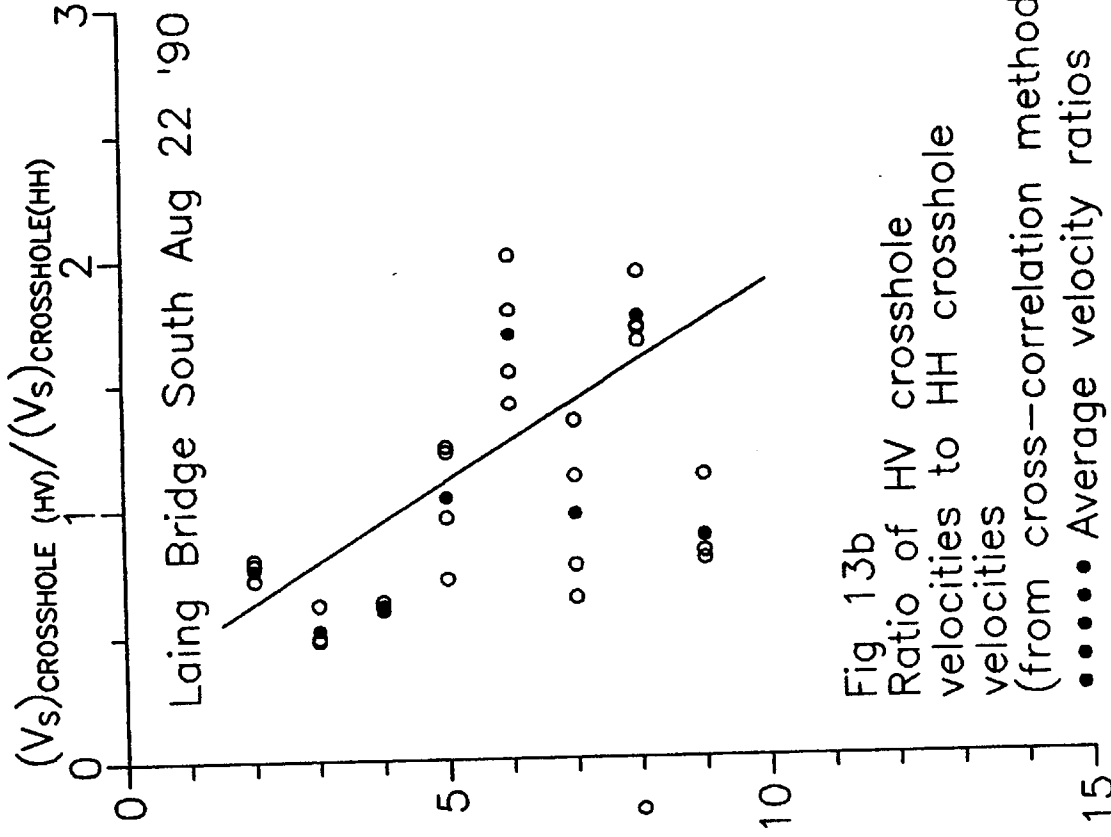


Fig 13a  
Ratio of downhole velocities  
to HH crosshole velocities  
(from cross-correlation method)  
●●●●● Average velocity ratios

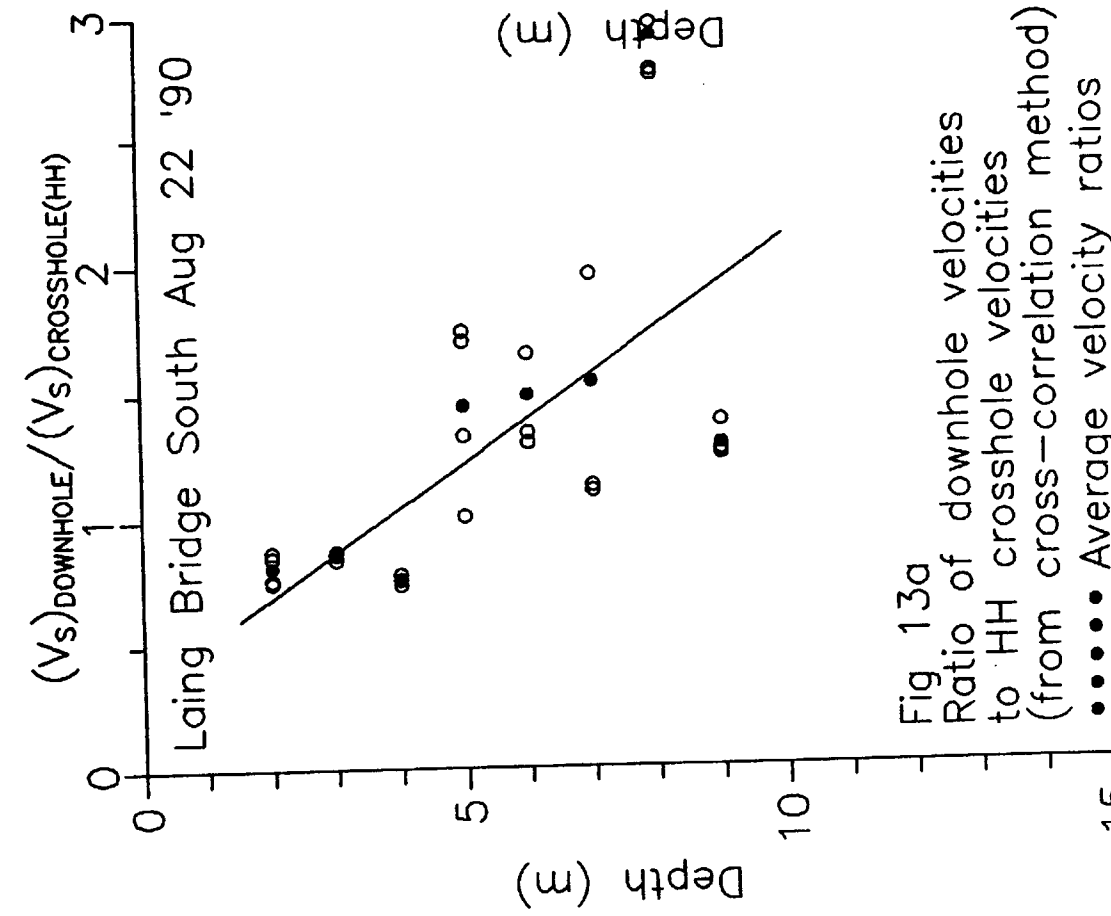


Fig 13b  
Ratio of HV crosshole  
velocities to HH crosshole  
velocities  
(from cross-correlation method)  
●●●●● Average velocity ratios

Figure 13b has a higher degree of scatter which makes interpretation difficult. Therefore, the data from figure 13a will be used for future analysis.

#### 5.1.4 - PLOT OF $K_0$ WITH DEPTH

Figures 14a and 14b show profiles of  $K_0$  with depth calculated from the stress equations defined in Chapter 3. The first item to note is that the stress equations are very sensitive to variations in the  $(V_s)_A / (V_s)_I$  ratio and hence cause some wide scatter in the profile. An interpretation of this data would suggest that the HV / HH velocity ratios have a wider variation in data than the downhole (VH) / HH velocity ratios. Both velocity ratio data give a high  $K_0$  value near the surface (in fact, the 2m and 3m values are right off the scale). The VH / HH velocity ratio plot in both Figure 14a and 14b then appears to become constant with depth at a low value. However, as stated above, the stress equations are very sensitive to the input data and these values of  $K_0$  are only a possible range.

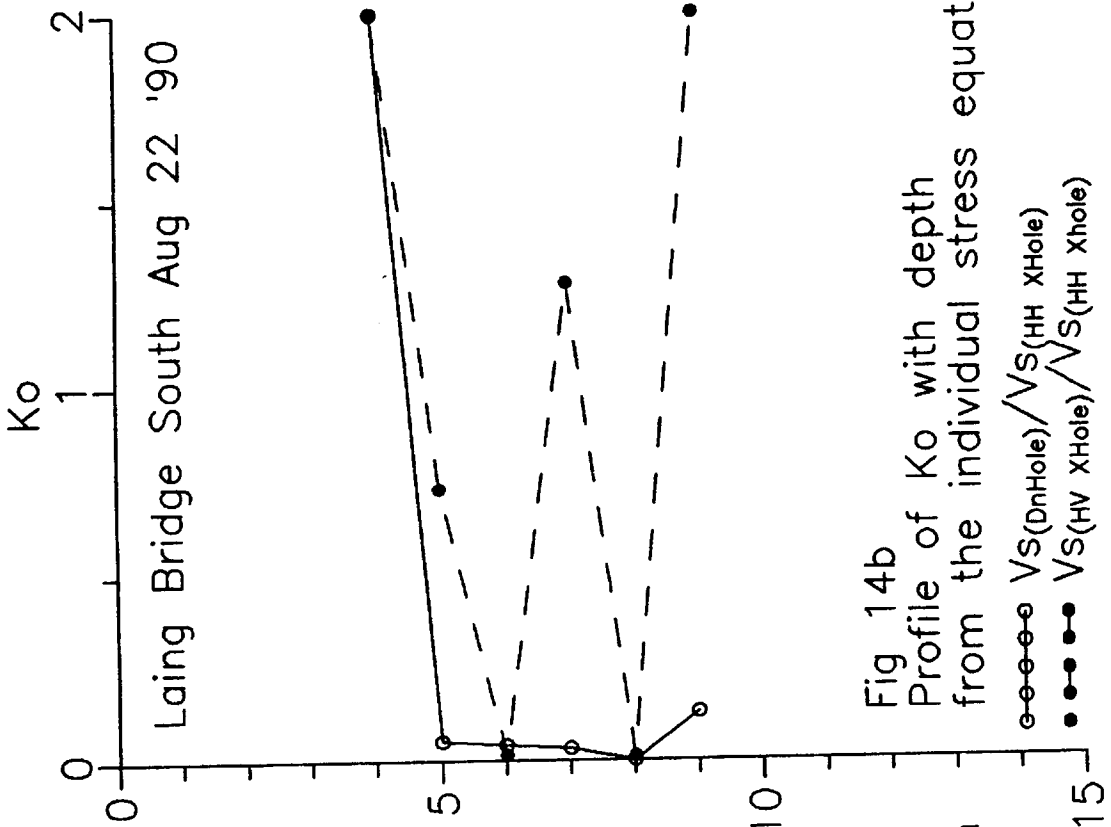


Fig 14a  
Profile of  $K_0$  with depth  
from the average stress equation

- $V_{S(DnHole)}/V_{S(HH \ xHole)}$
- $V_{S(HV \ xHole)}/V_{S(HH \ xHole)}$

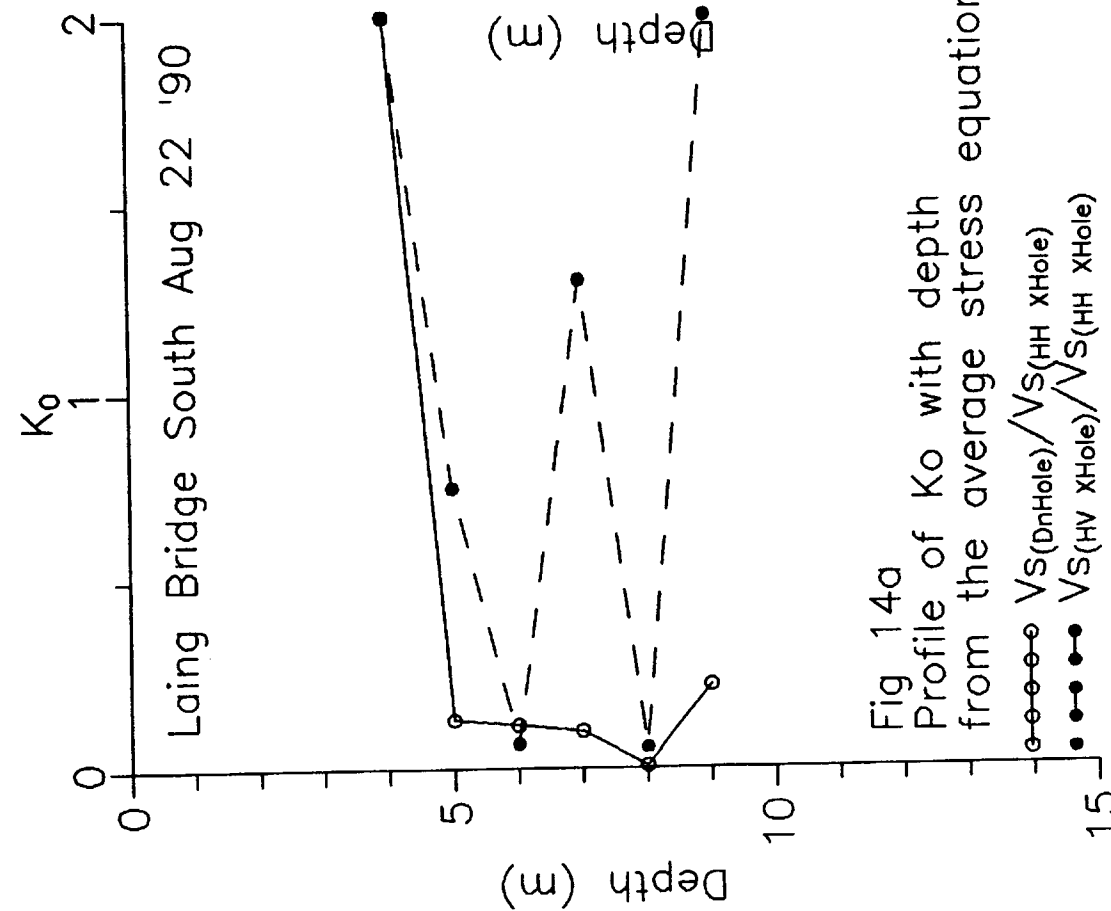


Fig 14b  
Profile of  $K_0$  with depth  
from the individual stress equation

- $V_{S(DnHole)}/V_{S(HH \ xHole)}$
- $V_{S(HV \ xHole)}/V_{S(HH \ xHole)}$

## 5.2 - 200th St. SITE

The results of the shear velocity calculations for this test site can be seen in the velocity versus depth graphs of figures 15 a-f.

### 5.2.1 - DOWNHOLE SEISMIC PROFILE

Looking at figures 15a and 15b, the plot shows that the shear velocities are high at the shallow depths (200 m/s - 300 m/s), and drop as depth increases, hitting a minimum value at 80 - 100 m/s at a depth of 6 - 7m. The velocities then increase linearly with depth to the end of the test. This profile suggests that the anisotropic stress conditions at shallow depths is very high, decreasing to a minimum at approximately 7m. The high stress conditions are most likely due to a previous load that was emplaced on the site, and is now removed. This result correlates well with the laboratory test results, which states that this site is overconsolidated to approximately 5 - 6m depth (Chap. 4). Once again, the cross-correlation data (Fig.15b) appears to have better grouping, although the trends given by both data sets are essentially the same. Therefore, the data from Figure 15b will be used in future discussions.

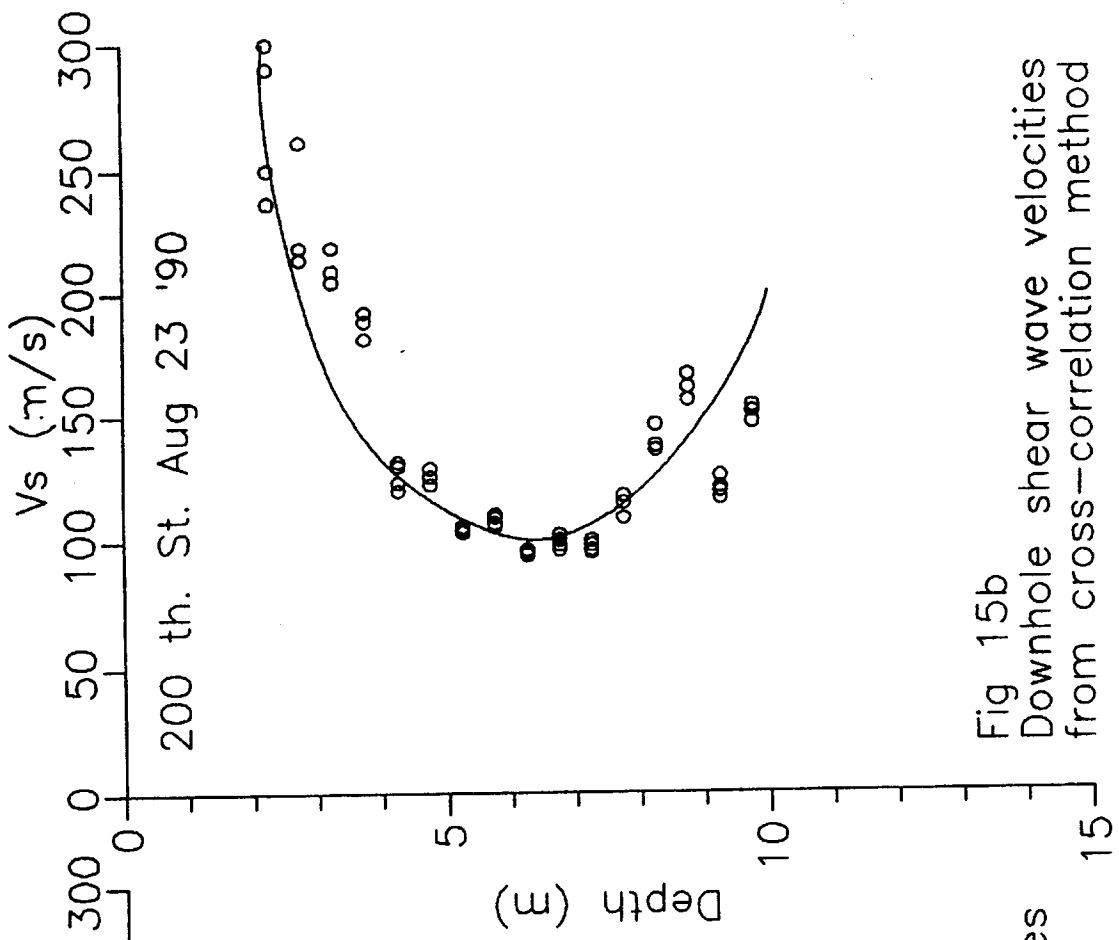


Fig 15a  
Downhole shear wave velocities  
from cross-over point

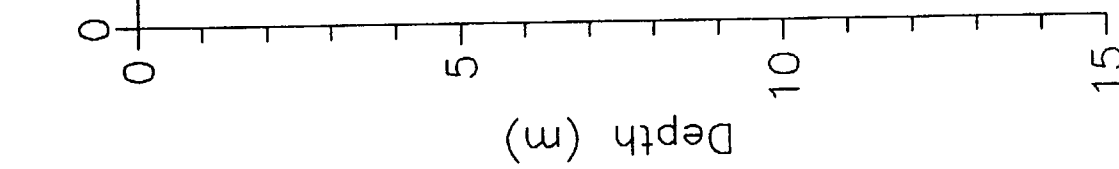


Fig 15b  
Downhole shear wave velocities  
from cross-correlation method

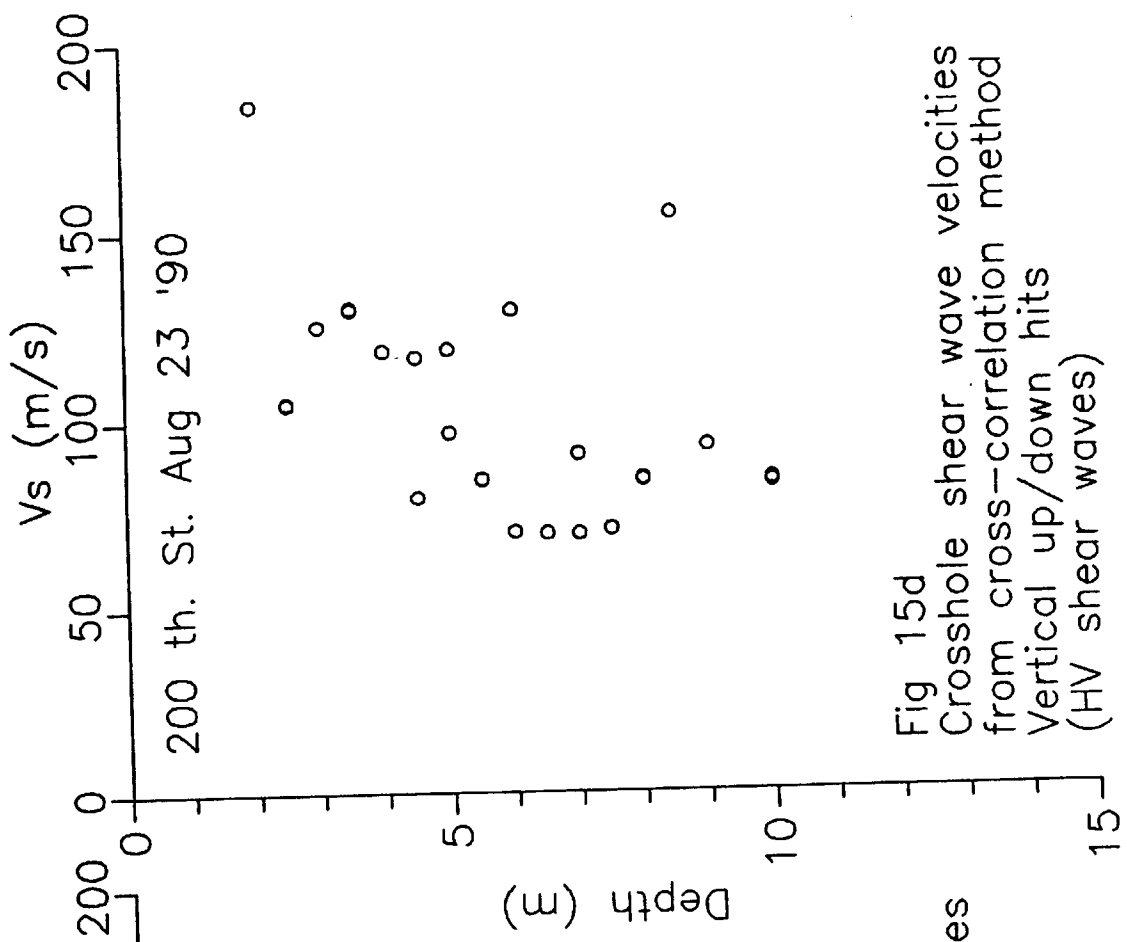


Fig 15c  
Crosshole shear wave velocities  
from cross-over point  
Vertical up/down hits  
(HV shear waves)

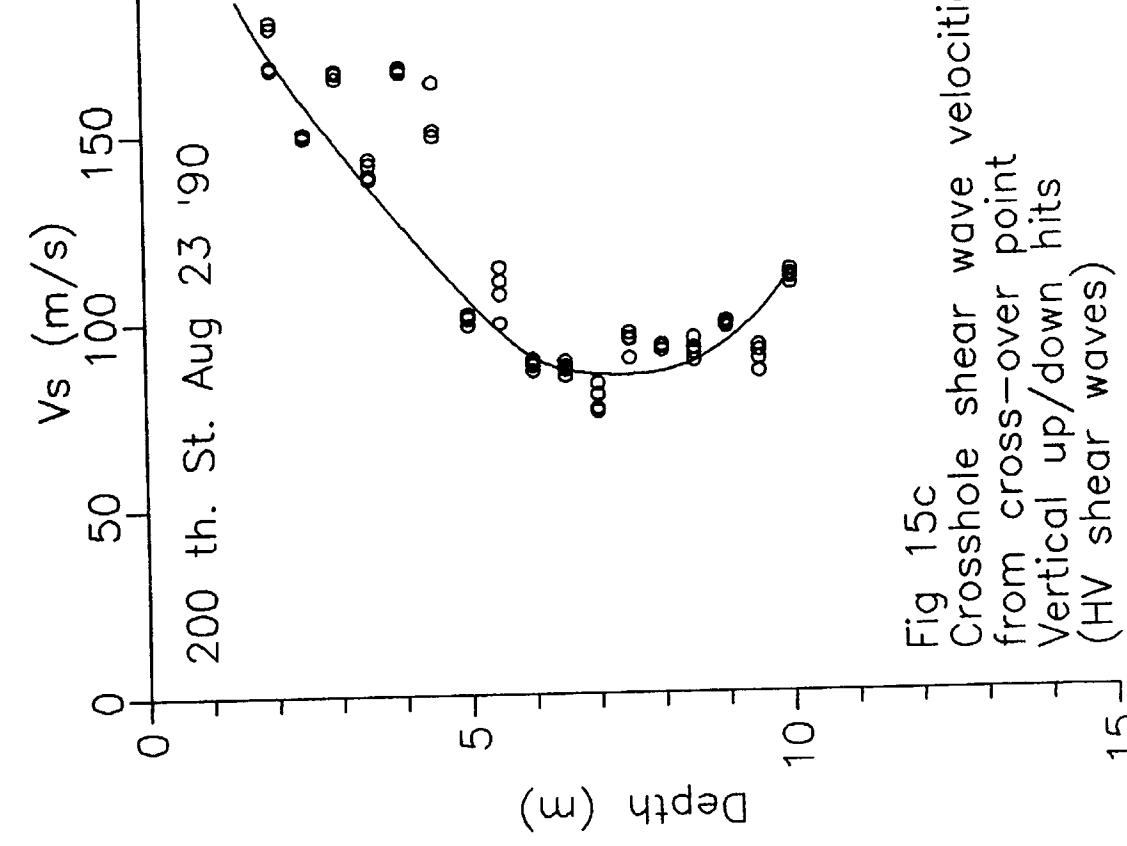


Fig 15d  
Crosshole shear wave velocities  
from cross-correlation method  
Vertical up/down hits  
(HV shear waves)

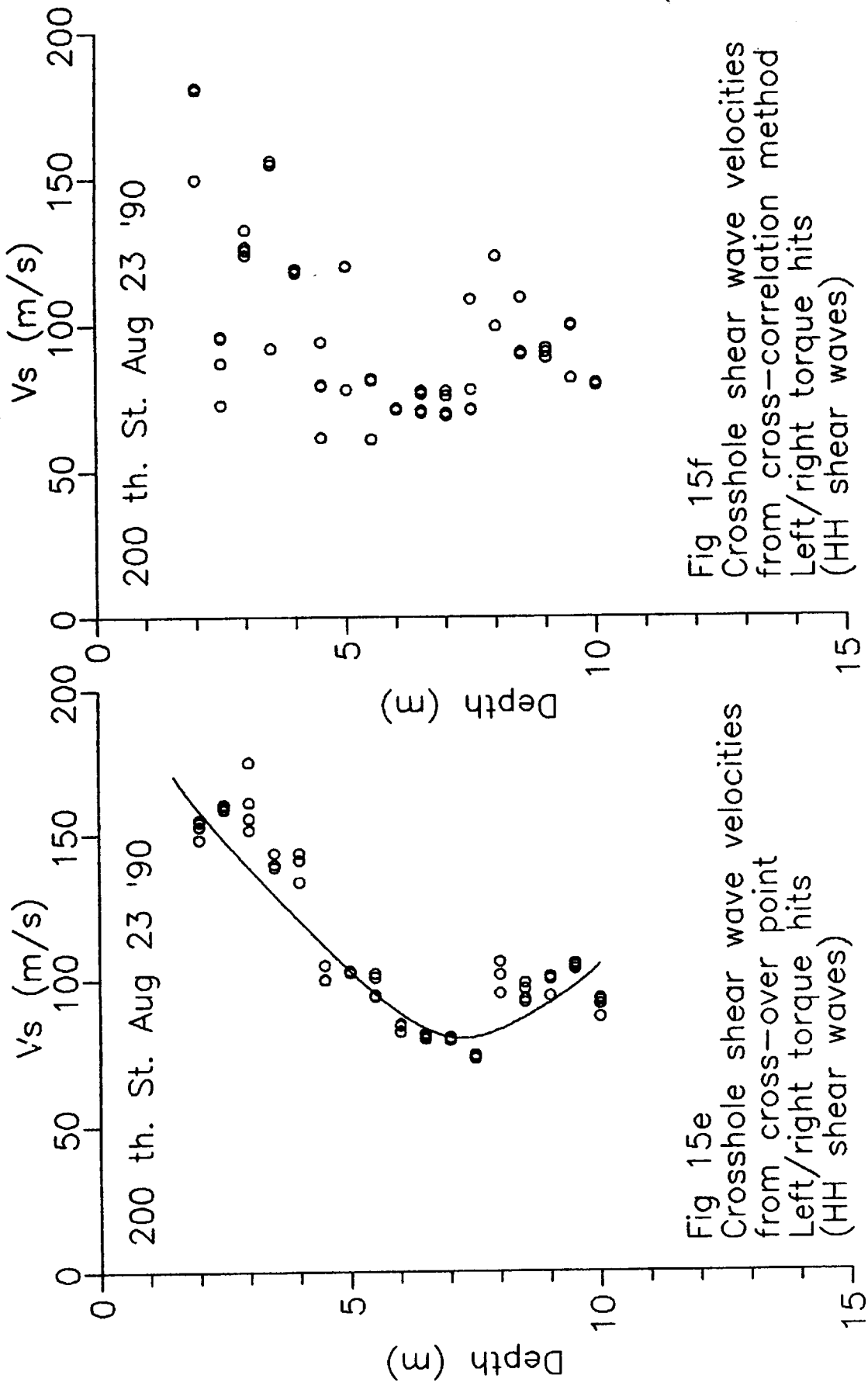


Fig 15e  
 Crosshole shear wave velocities  
 from cross-over point  
 Left/right torque hits  
 (HH shear waves)

Fig 15f  
 Crosshole shear wave velocities  
 from cross-correlation method  
 Left/right torque hits  
 (HH shear waves)

### 5.2.2a - CROSSHOLE SEISMIC PROFILE: HV SHEAR WAVE VELOCITIES

Looking at the HV shear wave plots with depth (Figs. 15c and 15d), the cross-over point data is much better grouped than the cross-correlation data. Up to now, it has been the cross-correlation data that has produced the more consistent results. This change in results may be explained by looking at a typical waveform signal generated at this site (Fig. 16). Normally, a typical seismic shear wave signal will show just one maximum peak, indicating the arrival of the shear wave. This peak is what the cross correlation method is trying to match with the maximum peak from the second receiver cone signal that is farther away from the source. However, if there is more than one maximum peak in the signal, the cross correlation method will try and match the two sets of maximum peaks in each signal as closely as possible, thereby not matching the two initial maximum peaks in each signal correctly, and altering the arrival time  $\Delta t$ , and hence the velocity.

The presence of a second maximum peak in the signal may be due to either reflections of the wave bouncing off a subsurface anomaly, such as a sand lens or sand layer, and returning to the receiver, or due to resonance or a "ringing" of the cone after

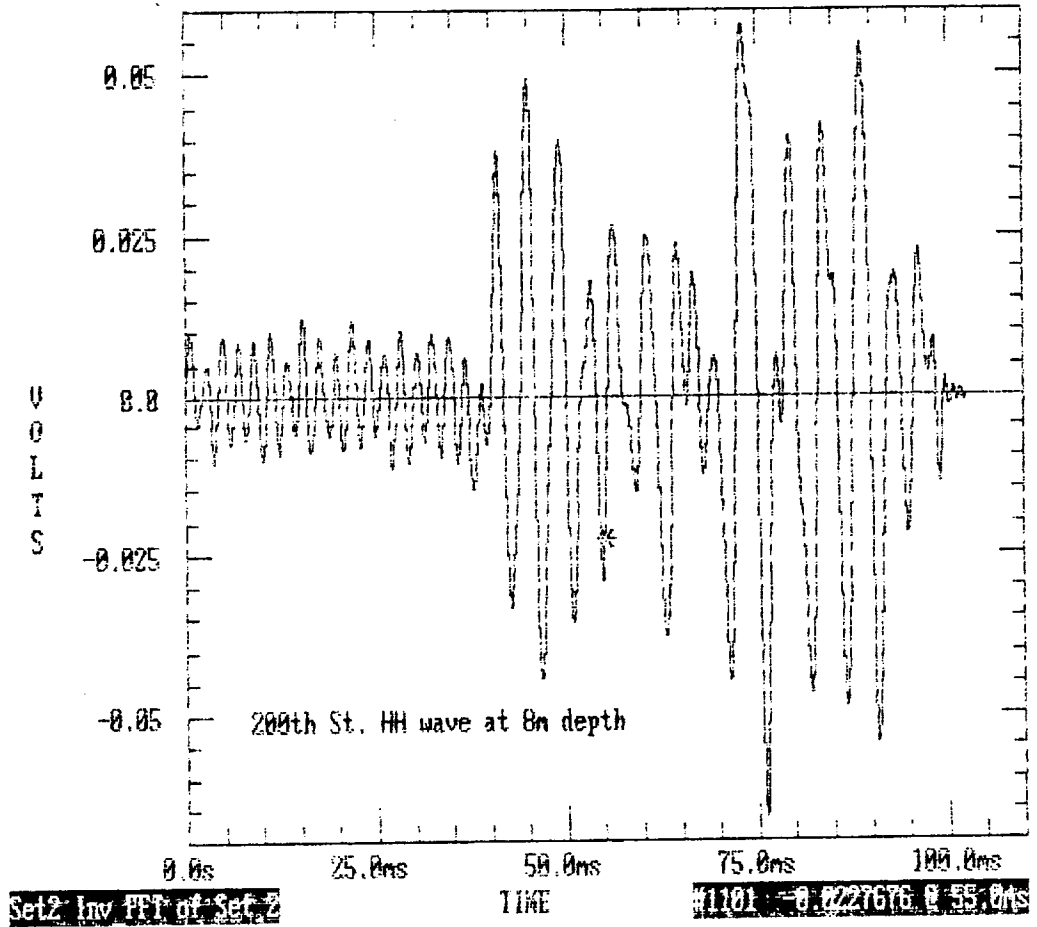


Fig 16 - Crosshole seismic generated signal from 200th St. showing two peaks

it has been hit, which would cause multiple shear waves to develop. Since it would have been very time consuming to remove the second wave signal from all the data (by windowing the data), and the crossover point method appears to have given very consistent results, the cross-correlation method data was left unchanged, and the cross-over data (Fig. 15c) will be used in future discussion.

The HV shear wave profile of Figure 15c is very similar to the downhole shear wave (VH) profile of Figure 15b, except that the shallow depth velocities do not start as high as the downhole profile. Since the HV shear wave velocities are related to the anisotropic stress conditions like the downhole shear wave velocities (Chap 3), similar velocity profiles are expected. However, the slight variation between the two profiles may be due to the fact that the downhole velocity profile averages the shear wave velocities over a 1m depth interval, while the crosshole velocity profile shows shear wave velocities that are calculated across a horizontal plane at one depth interval.

### 5.2.2b - CROSSHOLE SEISMIC PROFILE: HH SHEAR WAVE VELOCITIES

Looking at the HH shear wave velocity profiles (Figs 15e and 15f), again the cross-over point data is grouped better than the cross-correlation data, due to the same reason stated for the HV plots in the previous section. Therefore, the cross-over data (Fig. 15c) will be used for the preceding discussion.

The HH shear wave profile is virtually identical to the HV shear wave profile (Fig. 15c). This indicates that the stress conditions in the isotropic plane are much the same as the anisotropic stress conditions.

### 5.2.3 - COMPARISON OF VELOCITY RATIOS

Figures 17a and 17b relate the two anisotropic stress velocities to the isotropic stress velocities. Figure 17a shows the downhole velocity / HH crosshole velocity ratio to be high at shallow depths, decreasing to a minimum ratio of 1 at approximately 5m, and then increasing linearly with depth below 5m. An interpretation of this data would suggest that the soil is stiffer at shallow depths, decreasing to a minimum at 5m depth. The soil stiffness then increases linearly below 5m. This correlates well with the lab data results (Chap 4), which

states that the soil is overconsolidated at shallow depths to approximately 5 - 6m depth.

A comparison of the HV velocities to the HH velocities (Fig. 17b) shows a profile that is approximately constant with depth at a velocity ratio of about 1. This suggests that the HV velocity profile and the HH velocity profile are virtually

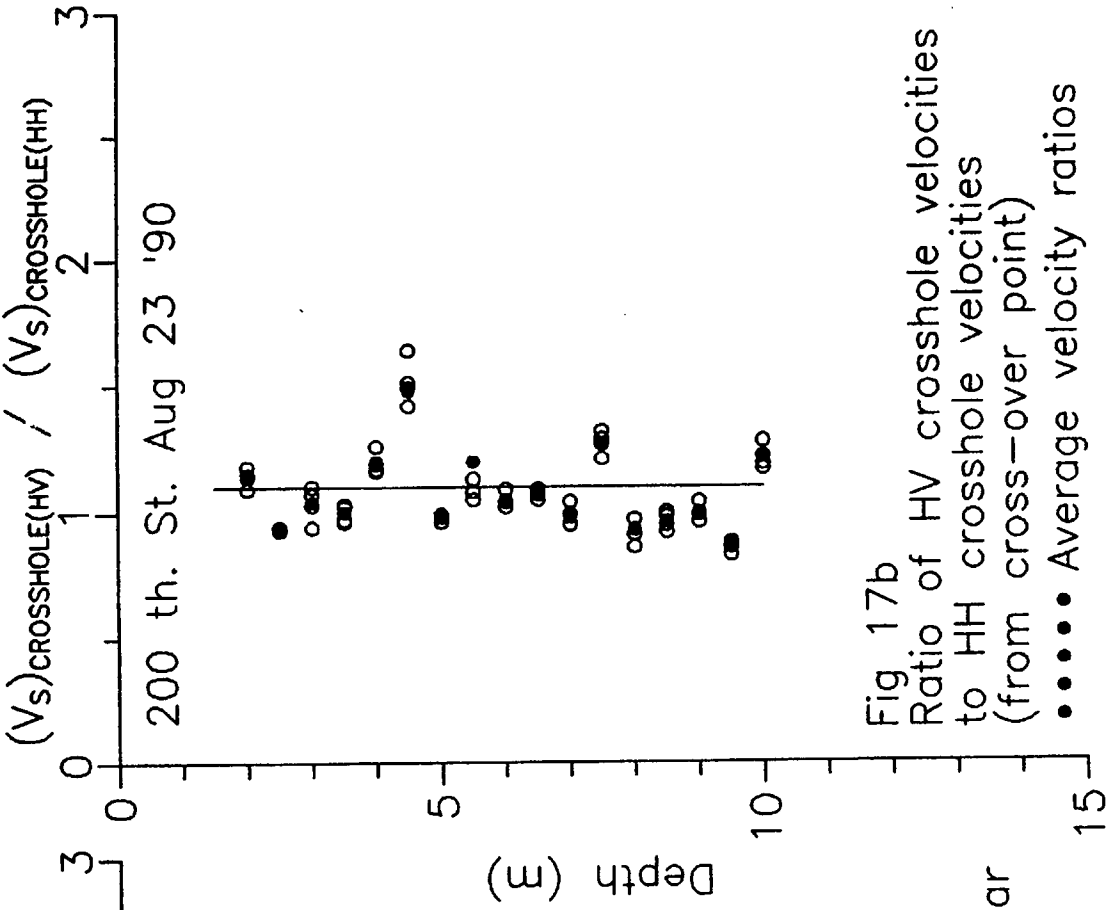


Fig. 17a  
 Ratio of downhole velocities  
 (cross-correlation) to HH shear  
 wave velocities (cross-over)  
 ●●●●● Average velocity ratios

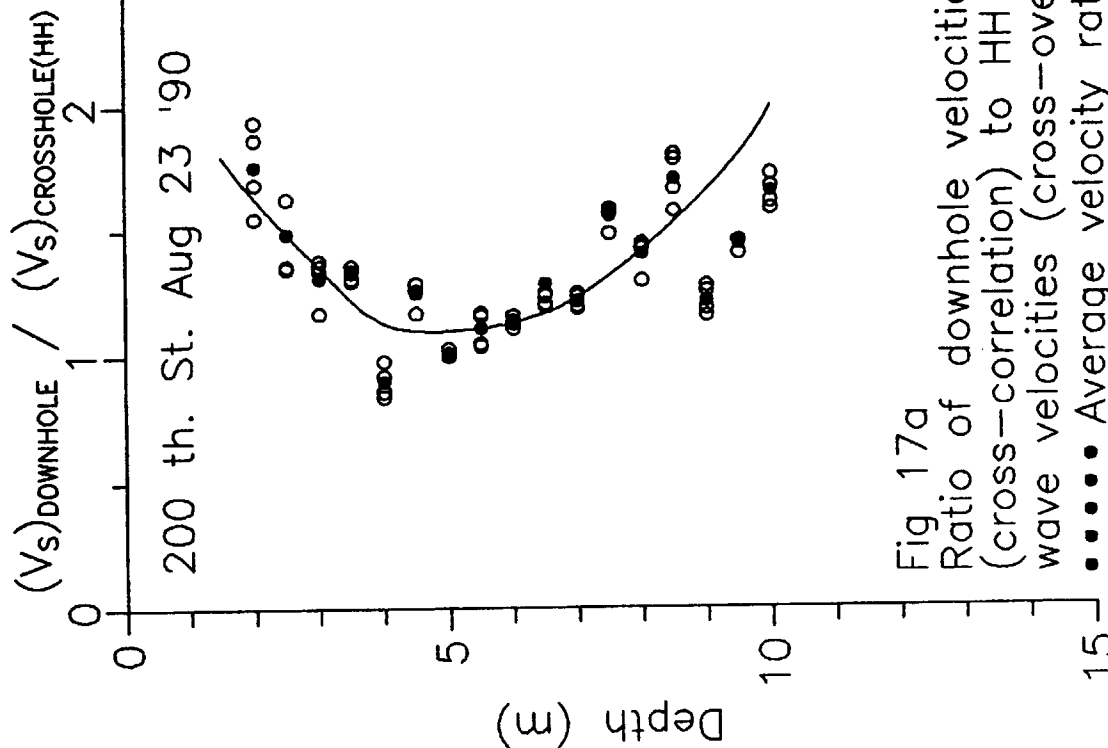


Fig. 17b  
 Ratio of HV crosshole velocities  
 to HH crosshole velocities  
 (from cross-over point)  
 ●●●●● Average velocity ratios

identical, which is what was noted in the previous section.

A conclusion from these two velocity profiles would be that relating the downhole shear wave velocities and the HH shear wave velocities shows a profile of the soil stiffness conditions with depth, while relating the HV and the HH shear wave velocities does not show an expected soil stiffness profile.

#### 5.2.4 - PLOT OF $K_0$ WITH DEPTH

Figures 18a and 18b show profiles of  $K_0$  with depth for this site. As stated in the results for the Laing Bridge Site, the stress equations are sensitive to the velocity ratio input, hence the wide scatter in the profile. It can be seen however, that the  $K_0$  profile done with the HV / HH velocity ratios has a much wider range of scatter than does the profile done with the downhole (VH) / HH velocity ratios. Noting back to the preceding section, it was found that the VH / HH velocity ratio profile with depth obtained a better description of the soil stiffness conditions at the site than did the HV / HH velocity ratio profile. Therefore, it can be assumed that the  $K_0$  profile done with the VH / HH velocity ratios would give a better estimation of  $K_0$ . In both Figures 18a and 18b, the

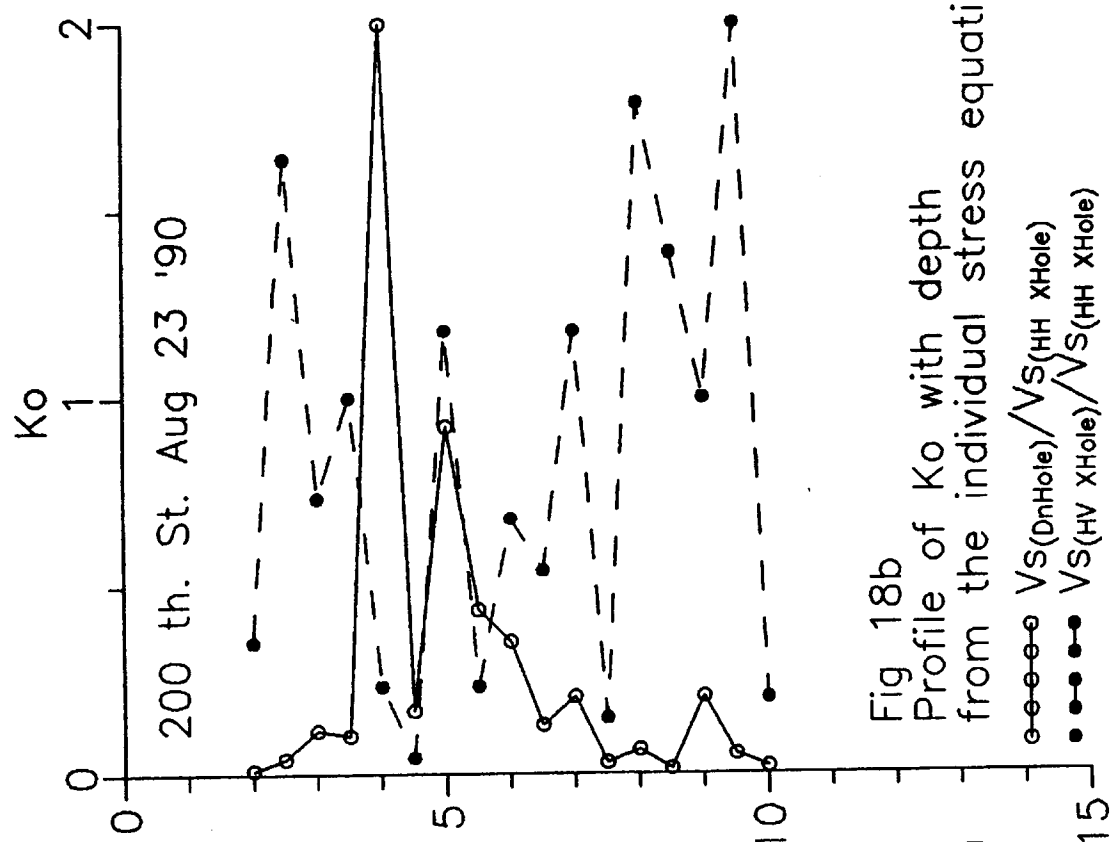


Fig 18a  
Profile of  $K_0$  with depth  
from the average stress equation

- $V_{S(DnHole)}/V_{S(HH xHole)}$
- $V_{S(HV xHole)}/V_{S(HH xHole)}$

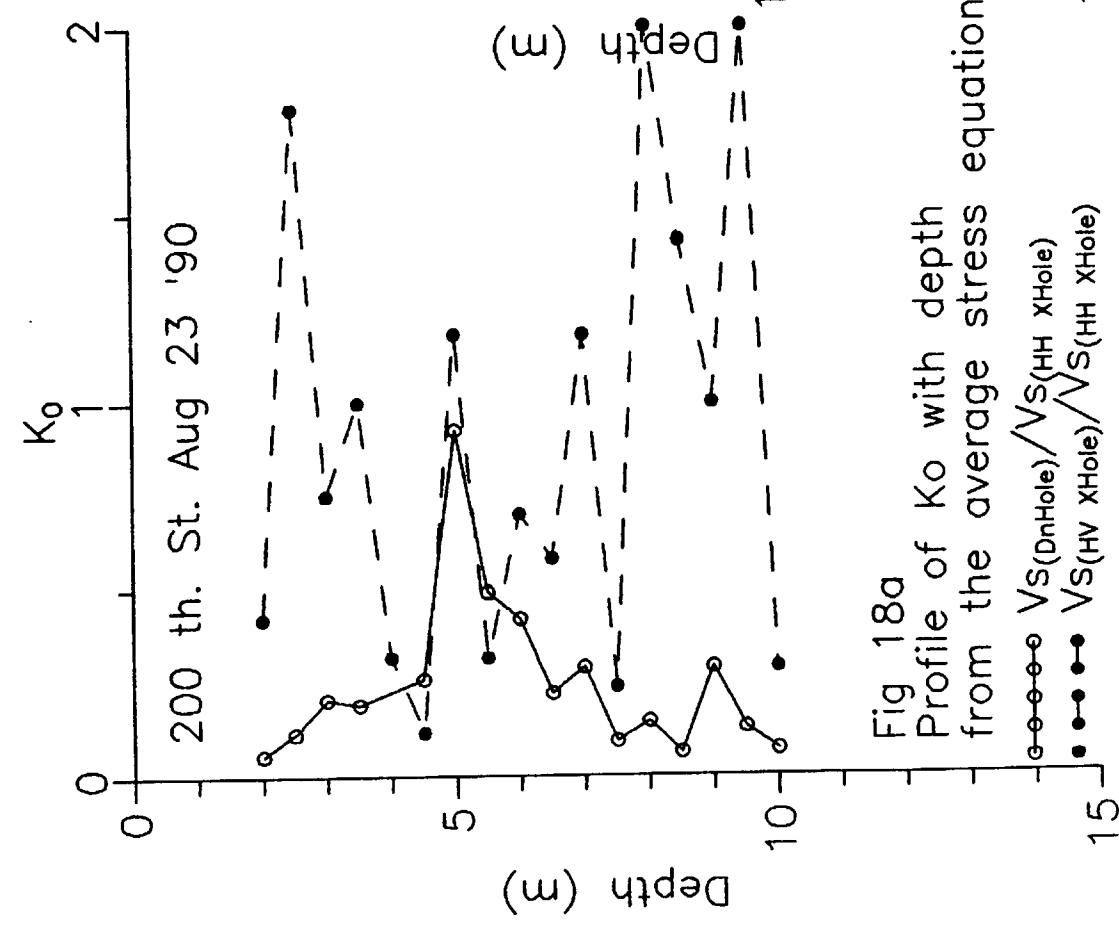


Fig 18b  
Profile of  $K_0$  with depth  
from the individual stress equation

- $V_{S(DnHole)}/V_{S(HH xHole)}$
- $V_{S(HV xHole)}/V_{S(HH xHole)}$

VH / HH velocity profile appears to increase slightly with depth to approximately 4 - 5m, then decrease below 5m depth. The HV / HH velocity profile has a wide amount of scatter as stated before, but the profile appears to be centered around a  $K_0$  value of one. This would be consistent with the results found in Figure 17b, in which the HV shear wave velocities appeared to be equal to the HH shear wave velocities. For this to be true,  $K_0$  would have to be equal to one, as defined by the equations in Chapter Three. However, as stated before, since the stress conditions are very sensitive to the velocity ratios, this is only a possible range for  $K_0$ .

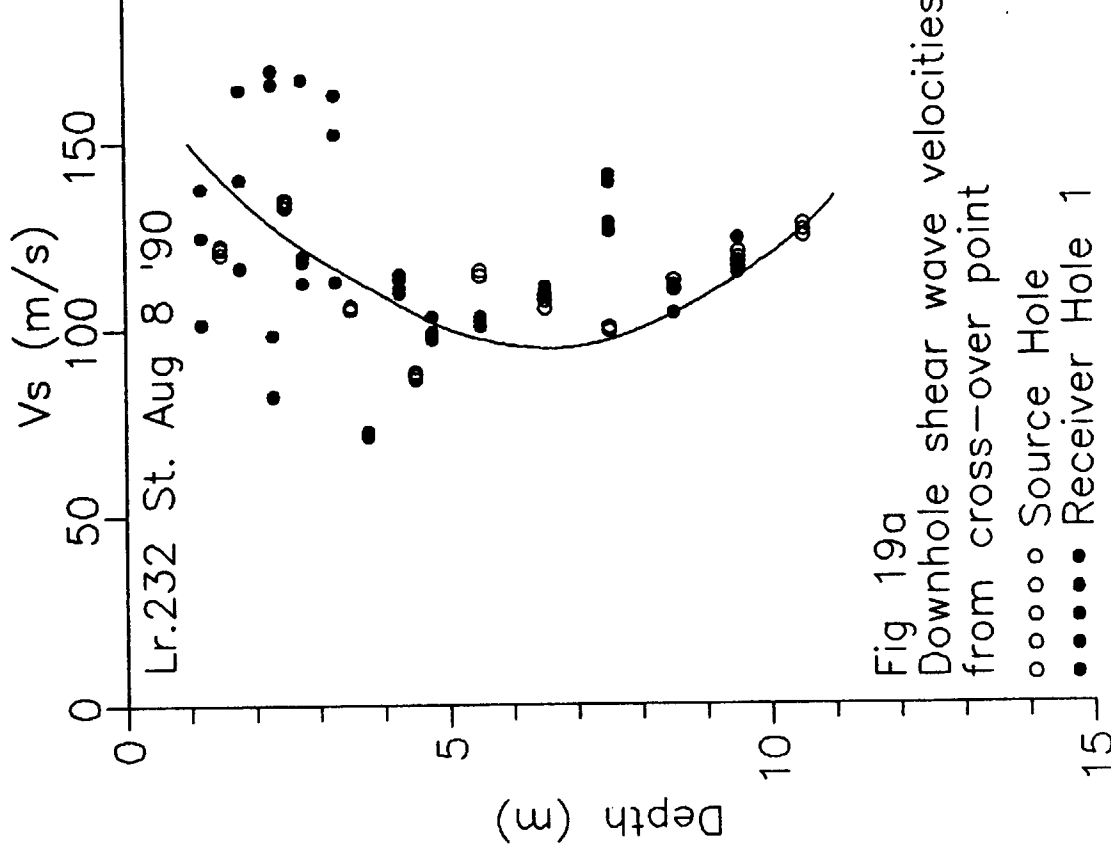
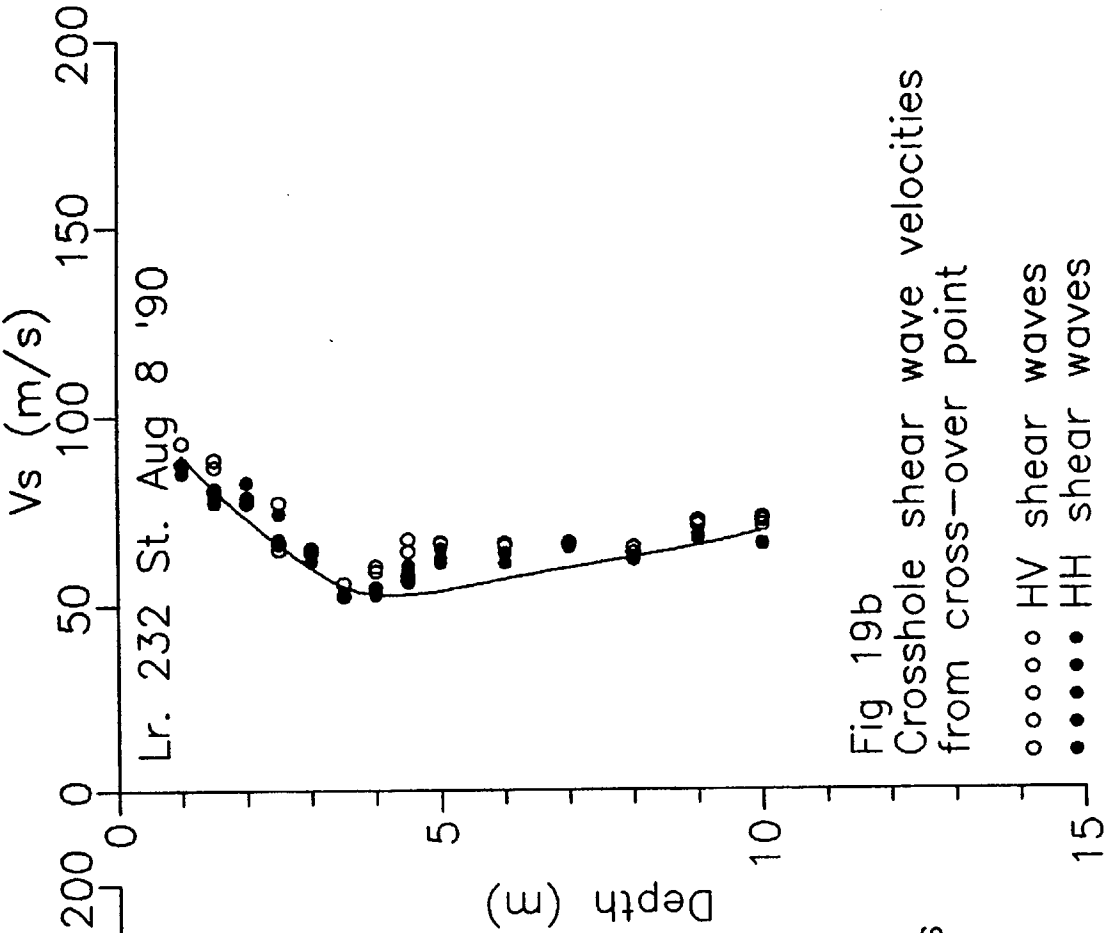
### 5.3 - 232nd St. SITE

During the field work for the acquisition of the downhole and crosshole seismic velocities for this site, one of the receiver cones was damaged. Therefore, the cross-correlation method of calculating shear wave velocity data (which requires two receiver cones for the crosshole seismic technique) could not be done. Consequently, the only velocity profiles available are the ones obtained from the cross-over point method. The downhole seismic method does not require two receiver cones, so

there was the possibility of obtaining a downhole seismic velocity profile from the cross-correlation method. To be consistent however, only the cross-over point profile is used for comparison against the crosshole seismic profiles. The profiles can be seen in Figures 19a and 19b.

#### **5.3.1 - DOWNHOLE SEISMIC PROFILE**

Figure 19a shows the downhole seismic velocity profile for the source hole (done while making a hole for the source cone) and the receiver 1 location. The two data sets coincide well with each other, and indicate high velocity values at shallow depth, decreasing to a minimum at approximately 4m, and



increasing linearly below 5m. This profile is very similar to the downhole seismic profile obtained at the 200th St. site (Fig. 15b), although the actual velocity values are less. Therefore, the interpretation could also be the same, which is; the anisotropic stress conditions are high at shallow depths, decreasing to a minimum at 5m depth, and increasing linearly below 5m. Since these two sites are very close to each other physically and have almost the same soil characteristics, it makes sense that the two downhole seismic profiles would be similar also.

### 5.3.2 - CROSSHOLE SEISMIC PROFILE

Figure 19b shows the crosshole seismic velocity profile for both the HV shear waves and the HH shear waves. The two profiles are nearly identical, and indicate slightly higher values at shallow depth, decreasing to a minimum at around 3 1/2m depth, and increasing slightly with depth below 4m.

### 5.3.3 - COMPARISON OF VELOCITY RATIOS

Figure 20a shows the ratio between the downhole seismic velocities and the HH shear wave velocities with depth. This plot is very similar to the downhole seismic velocity plot for this site (Fig. 19a). The velocity ratio is quite high at shallow depths, decreasing to a minimum at approximately 5m, and increasing linearly below 5m. An interpretation of this profile would be that the soil stiffness is high shallow depths. The soil stiffness decreases to a minimum at 5m, and increases again below 5m. This interpretation is identical to the one given to the 200th St. site (Chap 5.2.3). Since these sites are very similar physically, the interpretation of each site should be similar.

Figure 20b shows a plot of HV / HH velocity ratios with depth. The profile is constant with depth, with an average velocity ratio around one. This would suggest that there is no difference in the HV and HH velocities. Again, this is the same conclusion that was achieved for the 200th St. site.

A summary of this site would be identical to the 200th St. site. That is, the relation between the downhole shear wave velocities and the HH shear wave velocities gives a profile of

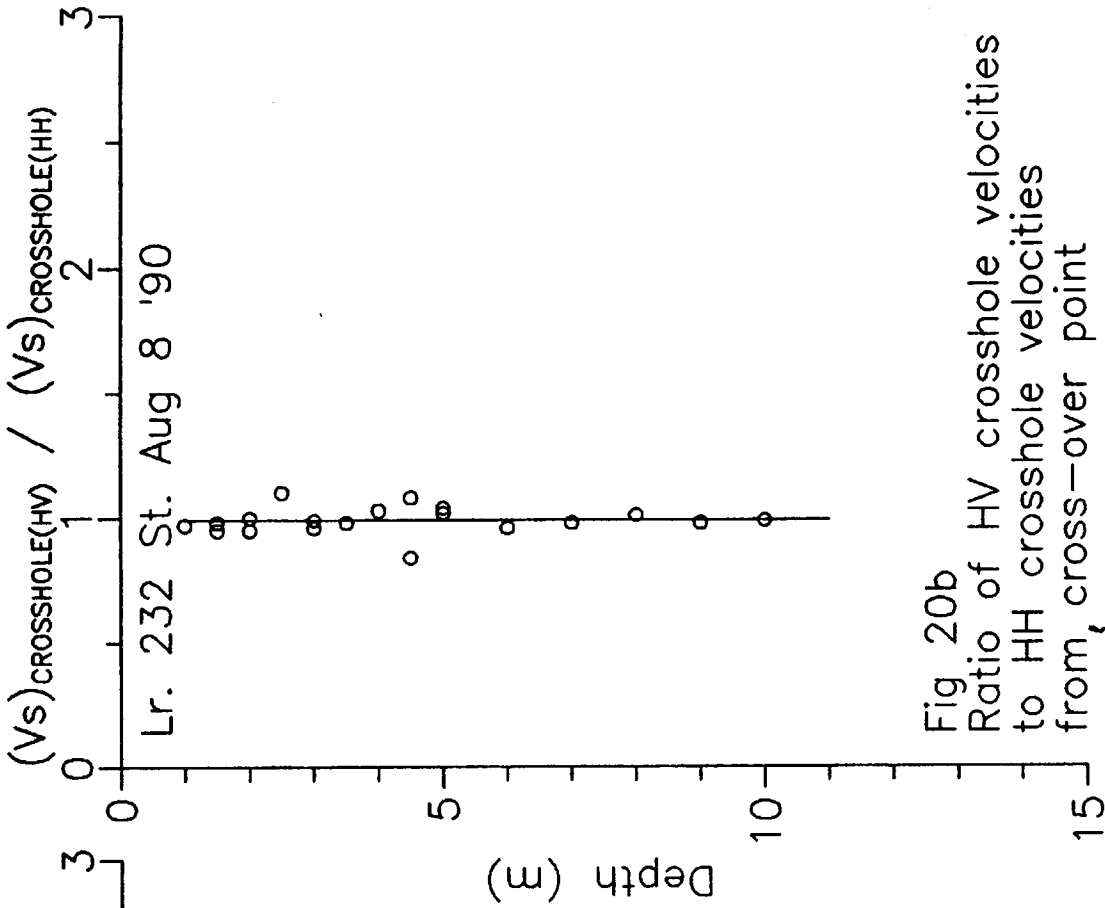


Fig. 20b  
Ratio of HV crosshole velocities to HH crosshole velocities from, cross-over point

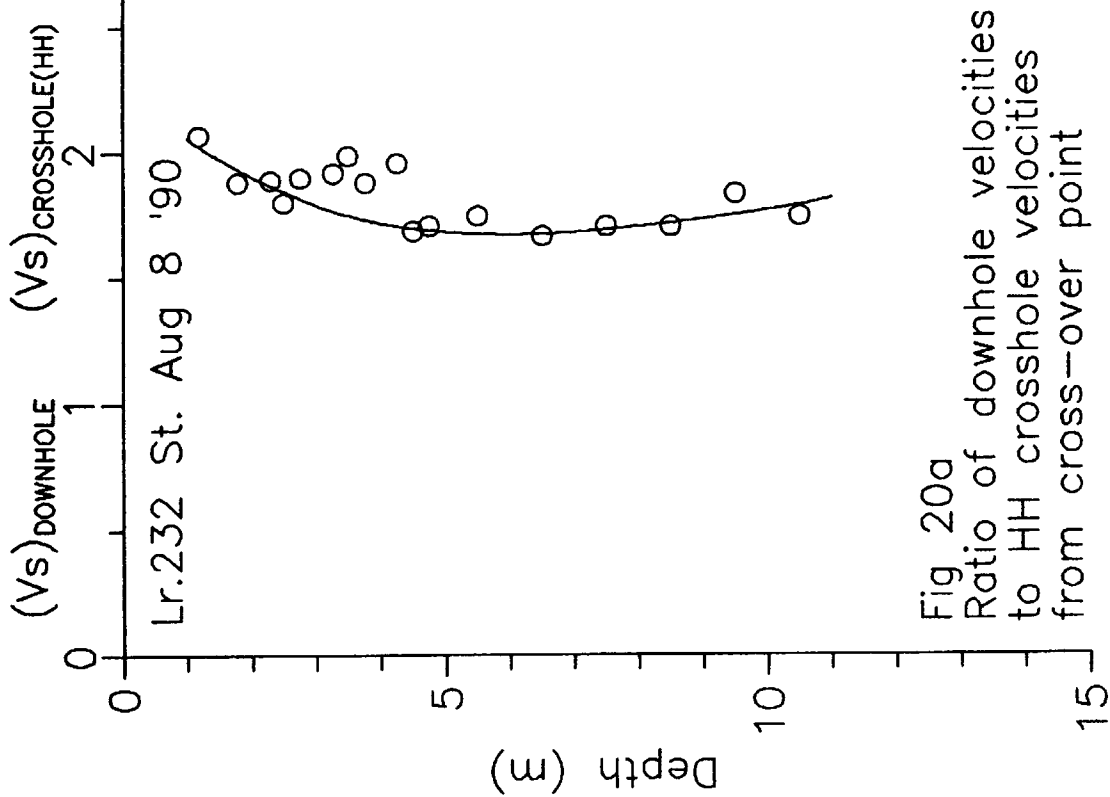


Fig. 20a  
Ratio of downhole velocities to HH crosshole velocities from cross-over point

the soil stiffness with depth, while the relation between the HV and the HH shear wave velocities produces no apparant soil stiffness profile at all.

#### 5.3.4 - PLOT OF $K_0$ WITH DEPTH

Figures 21a and 21b show the profile of  $K_0$  with depth. The profiles done with the downhole (VH) / HH shear velocity ratios appear to be almost consistent with depth at a very low  $K_0$  value. The profiles done with the HV / HH shear velocity ratios have a wide scatter, but appear to be centered around an average  $K_0$  value of one. The results from these two profiles are very similar to the results found from the  $K_0$  profiles of the 200th St. site. Since these two sites are physically close to each other, and laboratory tests indicate that the two sites have similar soil characteristics, it is feasable that the results from the two sites would be similar also.



CHAPTER SIXCONCLUSIONS

The results from the three sites tested indicate that it is possible to measure seismic shear wave velocities using the down hole seismic and crosshole seismic methods.

At the sand site (Laing Bridge South) the downhole (VH) shear wave velocity profile with depth indicates linearly increasing velocities with depth. The HV shear wave velocity profile from the crosshole method also obtains similar results. The HH shear wave velocity profile from the crosshole method again finds the velocities increasing with depth, but with a sharp change in the velocity profile at 4.5m. Ratios of the downhole (VH) / HH shear wave velocities with depth indicate that the velocity rates increase with depth.

At the two clay sites (200th St. and 232nd St.) the shear wave velocity profiles with depth indicate that the velocities are high at shallow depths, decreasing to a minimum at approximately 5m, and then increasing linearly below 5m. Ratios of the downhole (VH) / HH shear wave velocities with depth appear to give the same results. However, ratios of the HV / HH

shear wave velocities with depth appear to be constant with depth with a ratio value around one.

The results from the Laing Bridge South Site infer that the soil stiffness is increasing linearly with depth. Also, there may be a difference in the physical soil properties above and below 4.5m depths.

The results from the two clay sites indicate that the soil stiffness is high at shallow depths, decreasing to a minimum at approximately 5m depth and then increasing linearly below 5m. This would suggest that the two clay sites are overconsolidated above 5m.

Results from the  $K_0$  profiles with depth for all three sites indicate that the stress condition equations relating  $(V_s)_A / (V_s)_I$  to  $K_0$  are very sensitive to variations in the  $(V_s)_A / (V_s)_I$  ratio. Therefore, it is very difficult to obtain a  $K_0$  value from these profiles.

**REFERENCES**

- Campanella, R.G. and Robertson, P.K. 1984. A Seismic Cone Penetrometer to Measure Engineering Properties of the Soil. Soil Mechanics Series No. 84, Dept. of Civil Eng., U.B.C.
- Campanella, R.G. 1990. The Seismic Piezocone Penetration Test: A Practical Site Investigation Tool. Prepared for seminar on in-situ testing and monitoring, Etobicoke, Ont. Sept.
- Campanella, R.G., Baziw, E.J., Sully, J.P. 1989. Interpretation of Seismic Cone Data Using Digital Filtering Techniques. 12th Int. Conf. on soil mechanics and foundation engineering, Rio de Janeiro, Brazil, Vol. 1, pp 195-199
- Campanella, R.G. and Stewart, W.P. 1990. Seismic Cone Analysis Using Digital Signal Processing. 43rd. Canadian Geotechnical Conference, Quebec City, Que. Oct.

Campanella et al. 1990. Laboratory Index Tests on Fine Grained Soils From Two Lower Mainland Sites. Internal Data Report ISTG-1-90, Insitu Testing Group, Dept. of Civil Eng. U.B.C.

Canada Map Office 1977. Surficial Geology Map of New Westminster, B.C. Dept. of Energy, Mines and Resources, Ottawa, Map 1484A

Canada Map Office 1974. Surficial Geology Map of Vancouver, B.C. Dept. of Energy, Mines and Resources, Ottawa, Map 1486A

Lee, S.H.H. and Stokoe, K.H. 1985. Effects of Structural and Stress Anisotropy on Velocity of Low Amplitude Shear Waves Propagating Along Principal Stress Directions in Dry Sand. Report GR85-4, Civil Eng. Dept., Univ. of Texas at Austin (in progress).

Roesler, S.K. 1979. Anisotropic Shear Modulus due to Stress Anisotropy. Journal of the Geotechnical Eng. Division ASCE Vol 105, No. GT5 pp 871-880 July.

Stokoe, K.H. and Woods, R.D. 1972. Insitu Shear Wave Velocity by Cross Hole Method. The Journal of Soil Mechanics and Foundations Divisions, V.98, SM5. Proc. of the North American Soc. of Civil Eng.

Stewart, W.P. 1991. Phd Thesis in Progress. Civil Eng. Dept., University of British Columbia.

Sully, J.P. 1991. Phd Thesis in Progress. Civil Eng. Dept., University of British Columbia.

Yan, L. and Byrne, P.M. 1989. Simulation of Downhole and Crosshole Seismic Tests on Sand Using the Hydraulic Gradient Similitude Method. Soil Mechanics Series No. 132 Dept. of Civil Eng., University of British Columbia.